Agricultural Water Management 293 (2024) 108698

Contents lists available at ScienceDirect

Agricultural Water Management

journal homepage: www.elsevier.com/locate/agwat

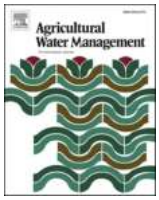

Enhancing reservoir operations with charged system search (CSS) algorithm: Accounting for sediment accumulation and multiple scenarios

Mohammad Abdullah Abid Almubaidin [a,b], Ali Najah Ahmed [c,d,*], Marlinda Abdul Malek [e], Moamin A. Mahmoud [f], Mohsen Sherif [g,i], Ahmed El-Shafie [h,i]

[a] Department of Civil Engineering, Khawarizmi University Technical College, Amman, Jordan
[b] Department of Civil Engineering, College of Engineering, Universiti Tenaga Nasional (UNITEN), 43000 Selangor, Malaysia
[c] School of Engineering and Technology, Sunway University, Bandar Sunway, Petaling Jaya, 47500, Malaysia
[d] Institute of Energy Infrastructure and Department of Civil Engineering, College of Engineering, Universiti Tenaga Nasional (UNITEN), Malaysia
[e] Department of Water & Environmental Engineering, Faculty of Civil Engineering, Universiti Teknologi Malaysia, 81310 Johor Bharu, Johor, Malaysia
[f] Institute of Informatics and Computing in Energy, Department of Computing, College of Computing and Informatics, Universiti Tenaga Nasional, Kajang 43000, Malaysia
[g] Civil and Environmental Engineering Department, College of Engineering, United Arab Emirates University, P.O. Box 15551, Al Ain, United Arab Emirates
[h] Department of Civil Engineering, Faculty of Engineering, University of Malaya (UM), 50603 Kuala Lumpur, Malaysia
[i] National Water and Energy Center, United Arab Emirates University, P.O. Box 15551, Al Ain, United Arab Emirates

ARTICLE INFO

Keywords:
Water resources management
Charged system search (CSS)
Reservoir operation optimization
Sediment simulation
Water deficit in reservoirs

ABSTRACT

Optimizing reservoir operation is a complex problem with non-linearities, numerous decision variables, and challenging constraints to simulate and solve. Researchers have tested various metaheuristics algorithms (MHAs) to reduce water deficit in reservoirs and presented them to decision-makers for adoption. Optimization methods vary depending on objectives, reservoir type, and algorithms used. The paper utilizes the CSS algorithm to study the impact of various scenarios on the optimal operation of the Mujib reservoir in Jordan to reduce water deficits using historical date between 2004 and 2019. The study explores different scenarios, including sediment impact, water demand management, and increasing the storage volume for the reservoir, to identify the optimal operation of the reservoir. The study compares the results of these scenarios with the current operation of the reservoir. Risk analysis (volumetric reliability, shortage index (SI), resilience, vulnerability) and error indexes (correlation coefficient R2, the root mean square error (RMSE), and the mean absolute error (MAE)) were used to compare results between scenarios, in addition to the annual water deficit values from the CSS algorithm for each scenario. The simulation of monthly sediment values in the Mujib reservoir showed that sediment accumulation accounts for 14.6% of the reservoir's volume at the end of 2019. Removing sediments retained by the dam can reduce water deficit by 19.42% when using the CSS algorithm. Additionally, reducing agricultural water demand by 11% and removing sediment reduced water deficit by 42.40%. The study also examined the impact of increasing the storage capacity of the reservoir by 10%, 20%, and 30%, revealing a decrease in water deficit by 35.44% when sediment removal was included in the analysis. The study examined the scenario of increasing the storage capacity of the Mujib reservoir by 30%, reducing water demand by 11%, and removing sediment. This scenario resulted in a 53.59% decrease in water deficit, providing decision-makers with viable solutions to address the water deficit problem in the reservoir.

1. Introduction

Reservoir operation optimization aims to balance diverse objectives, including ensuring water supply reliability, maximizing hydropower production, minimizing flood risk, and preserving the environment. Algorithms, considering constraints like storage capacity and inflow/outflow rates, play a pivotal role in this optimization process (Almubaidin et al., 2022; Zhang et al., 2019). Leveraging modern computing power enables these algorithms to process extensive data and offer real-time solutions for effective reservoir management (Asadieh and

* Corresponding author at: School of Engineering and Technology, Sunway University, Bandar Sunway, Petaling Jaya, 47500, Malaysia.
E-mail addresses: m.mubaidin@khawarizmi.edu.jo (M.A.A. Almubaidin), ale.a.najah@gmail.com (A.N. Ahmed).

https://doi.org/10.1016/j.agwat.2024.108698
Received 28 August 2023; Received in revised form 11 January 2024; Accepted 20 January 2024
Available online 2 February 2024

Afshar, 2019; Ashofteh et al., 2020).

Algorithms are vital for optimizing reservoir operations, determining optimal water release and managing inflow and outflow (Bozorg-Haddad et al., 2018). Sediment calculations, crucial for assessing capacity and lifespan, help estimate deposition, erosion, and transport. Addressing sedimentation is essential, considering risks like reduced storage, water quality compromise, and impaired hydraulic structure functionality (M. A. Almubaidin et al., 2023; Chamoun et al., 2016). These calculations contribute to effective reservoir management and long-term operational efficiency. Algorithms, incorporating sediment calculations, assist in formulating release strategies, aiding water managers in balancing competing demands and ensuring the reservoir's sustainability (Hajiabadi and Zarghami, 2014; Khan et al., 2012; Yin et al., 2014).

The optimization of reservoir operations presents a complex challenge characterized by non-linear functions, numerous decision variables, and multiple constraints (Chong et al., 2021). Historically, researchers have explored diverse metaheuristic algorithms (MHAs) to enhance water supply operations in reservoirs, addressing goals like minimizing water deficits and maximizing the utilization of released water from dams (Zhang et al., 2019). The optimization methods employed differ based on objectives, reservoir types, and the specific algorithm utilized (M. A. A. Almubaidin et al., 2022). Various MHAs have been employed and developed for this purpose, including: genetic algorithm (Ashofteh et al., 2021; Mendoza Ramírez et al., 2021), artificial bee colony (Moeini and Soghrati, 2020), particle swarm optimization (Bayesteh and Azari, 2021), grey wolf optimizer (Donyaii et al., 2020), crow algorithm (Banadkooki et al., 2020), spider monkey algorithm (Ehteram et al., 2018), shark algorithm (Allawi et al., 2018), firefly algorithm (Patle et al., 2017), krill herd algorithm (Karami et al., 2018), bat algorithm (Jamshidi and Shourian, 2019), Jaya Algorithm (Kumar and Yadav, 2020), Water Cycle Algorithm (Qaderi et al., 2018), Charged System Search (Asadieh and Afshar, 2019), and invasive weed optimization algorithm (Kalhori et al., 2023; Moghadam et al., 2022).

The challenge faced by decision-makers in reservoir management is the inadequate availability of data concerning the gradual accumulation of sediments over time. This limitation hinders the accurate monthly simulation of sediment levels, despite their substantial impact on the reservoir. The scarcity of data stems from irregular sediment sample collection or reliance on remote sensing techniques (Cimorelli et al., 2021; Su et al., 2022). Additionally, valuable data sources like water inflow, erosion rates, and watershed land use changes, which can influence sedimentation, remain underutilized (Shi et al., 2019). The deficiency in sediment accumulation data poses a significant hindrance for decision-makers striving to make well-informed choices regarding reservoir system management.

The examined rainwater-dependent reservoirs, typically located in arid regions, face a significant challenge in water management. Relying on unpredictable storms for inflow, these reservoirs experience varying monthly and annual water inflows, impacting storage and leading to losses from evaporation, seepage, and sedimentation. While demand remains constant, optimizing operation becomes crucial (Md. Azamathulla et al., 2008). Algorithms simulating reservoir behavior offer optimal solutions to navigate these challenges, considering variables like sediment, water demand, and storage capacity.

The study aims to simulate monthly sediment volume in the Mujib reservoir using the linear regression method and measured values. Additionally, it seeks to reduce water deficits through the CSS algorithm, considering scenarios like sedimentation impact, water demand, and increased storage. Simulations will identify effective strategies for sediment management, water optimization, and enhanced storage. The CSS algorithm is expected to significantly decrease water deficits, ensuring a sustainable water supply. Evaluation criteria include annual deficit values, risk analysis (reliability, resilience, and vulnerability), and error indices like mean absolute error (MAE), the root mean square error (RMSE), and the correlation value R2.

2. Materials and methodology

2.1. Sedimentation calculation

One of the main challenges that dams around the world encounter is the accumulation of sediment behind them. As water inflows from the upstream watersheds into the reservoir, it causes erosion of the drainage area, resulting in the deposition of sediment either upstream of the reservoir or in the calm waters of the reservoir, which may affect the storage capacity of the dam or reduce the ability to Hydroelectric power production, which reduces the life of the reservoir (Ijam et al., 2020). And because these sediments greatly affected this dam, it was necessary to enter them into the reservoir simulation system, and for that, the Mujib reservoir's cumulative sediment impact was simulated using the Modified Universal Soil Loss Equation (MUSLE) model. The MUSLE model, which is widely used for soil erosion prediction, is actually an improved version of the Universal Soil Loss Equation (USLE) (Benavidez et al., 2018).

The model will be calibrated and verified using the cumulative sediment yield data obtained from Eco-sounder device obtained from the Dams Directorate in the Jordanian Ministry of Water and Irrigation and the MUSLE model is expressed as in Eq. (1) (Williams, 1975). also expressing the steps of using this equation in Fig. 1.

$$Y = 11.8\left(Q.q_p\right)^{0.56}(K)(C)(P)(LS)(CFRAG) \quad (1)$$

Where Y is sediment Yield (Tones); q_p is peak flow rate (m^3/s); Q is water runoff (m^3); C is the cover management factor (dimensionless); K is the soil erodibility factor (MJ-1 mm-1); LS is the slope length and slope steepness (dimensionless); P is the erosion control practice factor (dimensionless); $CFRAG$ is the coarse fragment factor (dimensionless).

2.2. Surface runoff and peak flow rates

Runoff refers to the volume of water discharged from a specified drainage basin over a specific period. The maximum flow rate of runoff that occurs during a particular rainfall event is referred to as the peak flow rate (q_p). It is an important parameter that indicates the erosive power of the storm and is often used as a predictor of sediment loss (Neitsch et al., 2011).

The Mujib Dam's daily surface runoff volume values spanning from November 2003 to December 2019 were acquired from Jordan's Dams Directorate, Ministry of Water and Irrigation. However, to calculate the peak runoff rate, it was essential to determine the time of concentration (Tc) for the Al-Mujib catchment area. The Soil Conservation Service (SCS) formula was employed for this calculation, with parameters obtained through the Watershed Modelling System (WMS) 10.1 software. A digital elevation map (DEM) with a 30-meter resolution was extracted using Global Mapper 19 software. After WMS software utilization, the catchment area of the Mujib Basin exhibited an average slope of 5.67%, a hydraulic length of 185.90 km, and a weighted curve number (CN) of 89.07, sourced from a relevant study within the same area (Ijam and Al-Mahamid, 2012). Then lag time of 16.43 h and a time of concentration of 27.39 h.

2.3. Soil erodibility factor and coarse fragment factor (CFRG)

Soil erosion (K) indicates the rate at which soil particles are separated and transported due to the quantity and velocity of runoff during a specific storm event (Farhan and Nawaiseh, 2015). CFRG expresses the percentage of rocks in the upper soil layer from the percentage returned for each soil sample on sieve No. 4 and sieve No. 10 (Neitsch et al., 2011).

Ijam et al. (2020) gathered 21 soil samples from various points within the Mujib basin to assess soil erodibility factors (K) and the Coarse Fragment Factor (CFRG). The average K value obtained was

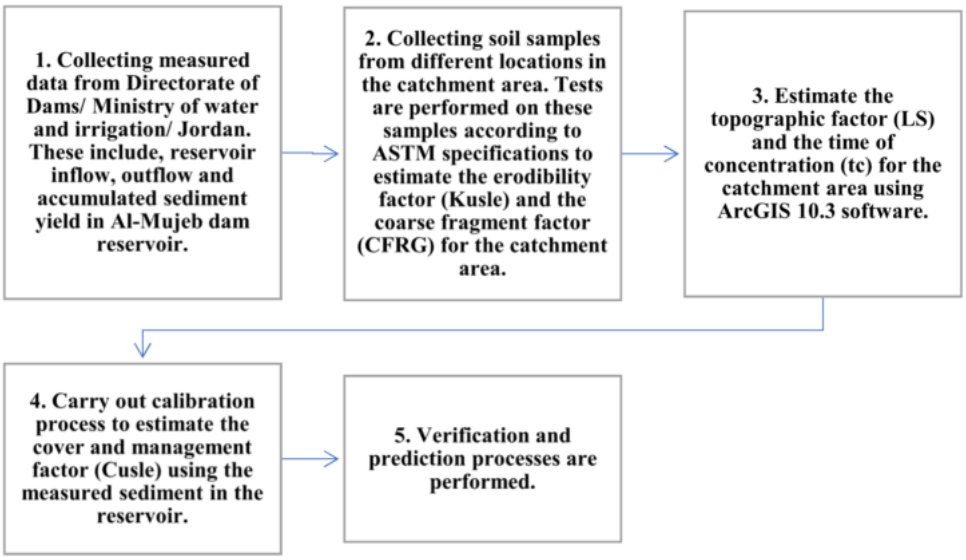

Fig. 1. Steps for calculating sedimentation amounts in Mujib Dam, according to the available data.

0.164. According to the soil classification triangle, the soils in the catchment area are classified as silt loam to loam soils. The average CFRG value recorded was 0.384.

2.4. The support practice factor (PUSLE)

Practices that support erosion control typically involve redirecting runoff away from slopes prone to erosion or slowing it down to minimize sedimentation. Examples of such practices include concave slopes, vegetation strips, and terraces. The effectiveness of a conservation practice in reducing soil erosion can be determined by the value of *P*, with lower values indicating more effective erosion control. In the absence of supporting practices, erosion control may be insufficient, the factor *P* is 1 (Arekhi et al., 2012). In this study, the support exercise factor (P) is presumed to be 1, as no measures have been implemented to mitigate ground erosion in the catchment area.

2.5. The slope length L and slope steepness S

The *LS* factor help to show the effective topography in the erosion model in MUSLE where the increase in the slope length *L* leads to an increase in the erosion due to the gradual accumulation of runoff in the along of the downward slope and the increase in the slope steepness factor *S* leads to an increase in soil erosion and thus an increase in the erosion speed (Khassaf and al Rammahi, 2018). The *LS* factors are measures of the potential for soil loss on a given slope length and steepness to soil loss from a slope of 72.6 feet in length and 9% steepness where all other conditions are identical (Wischmeier, 1978).

The slope length factor *LS* was calculated by using ArcMap10.3 software and using unit stream power erosion and deposition model (USPED) by following the steps used in Ijam et al. (2020), where the average *LS* value is 265.137.

2.6. Cover management factor (C)

The C factor is a measure of the ratio of soil loss under a specific land use condition relative to that of the base soil and ranges from 1 in bare soil, 1–9/10 in root crops and tubers, 1/1000 in forests, 1/100 in grasslands, and cover plants. *C* is a sensitive value for soil erosion because it is directly proportional to soil erosion, so the C factor is a useful parameter for calibrating sedimentation models and conducting soil erosion studies (Bekele, 2021; Ijam et al., 2020).

The value of the land cover and management factor (*C*) remains in the Eq. 1. It will be used to calibrate a MUSLE model regarding sediment productivity in the Mujib Dam reservoir to find the monthly sediment quantity to be used in the reservoir simulation system.

2.7. Case study: Mujib reservoir

The Mujib reservoir holds significant importance in Jordan as it serves various purposes such as domestic use, irrigation, and industrial operations. Its construction was completed in 2003, and it has a height of 62 m, a storage capacity of 31.2 MCM, and relies on a water catchment area of 4408.5 km. The reservoir receives an average annual inflow of 22.23 MCM of water, and its primary objective is to harness and conserve excess rainfall water in the Mujib Basin's catchment areas. This reservoir of water is stored in the reservoir, ensuring its availability for future use. Fig. 2 displays the catchment region of the Mujib reservoir. This type of reservoir experiences significant fluctuations in daily, monthly, and yearly inflow, as well as variable evaporation rates that are determined by the surface area of the reservoir. Unfortunately, sediment accumulated under the dam is a persistent problem, which leads to reduced storage capacity in the future and lower overall efficiency of the reservoir (Ijam et al., 2020).

A study was conducted using historical data on the monthly inflow for the Mujib reservoir from 2004 to 2019. This data was collected from the Jordanian Ministry of Water and Irrigation and analysed to obtain information on the average monthly evaporation rate and statistical values for the average monthly inflow in the reservoir. The results of this analysis are shown in Table 1.

2.8. Reservoir operation optimisation

2.8.1. Charged system search algorithm

Similar to numerous meta-heuristic methods that draw inspiration from natural phenomena, the CSS algorithm relies on the well-known Coulomb's law of electrostatics and the laws of motion from Newtonian mechanics developed in 2010 (Kaveh and Talatahari, 2010). The CSS algorithm contains agents called charged particles (CPs) and considers each CP as a charged sphere having a uniform charge density that can be imposed by an electrical force on other CPs according to Coulomb's law (Asadieh and Afshar, 2019; Kaveh and Talatahari, 2010). The attractive force between CP varies depending on their separation distance (Kaveh and Talatahari, 2010).

After calculating the net force acting on each CP, Newton's law is applied to determine the acceleration of each CP. Newtonian mechanics

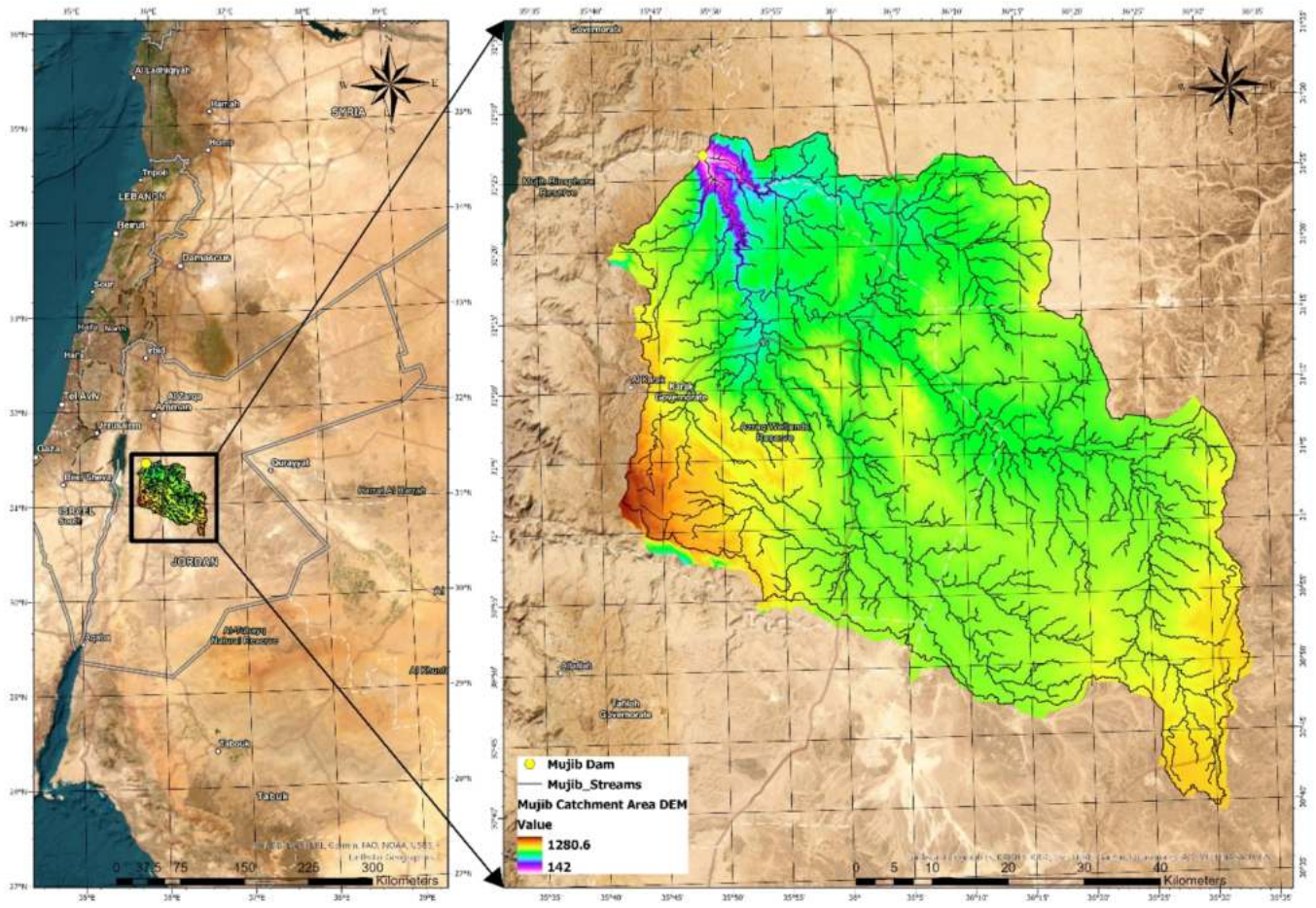

Fig. 2. The catchment area of Mujib Reservoir.

Table 1
The Mujib reservoir's monthly hydrological data.

Month	Average Evaporation rate monthly (m)	Average inflow (MCM)	Standard deviation	Maximum Inflow (MCM)
January	0.054	5.28	8.80	30.58
February	0.066	5.17	7.23	25.26
March	0.138	2.91	5.97	18.53
April	0.229	4.48	16.03	64.50
May	0.291	0.38	1.51	6.02
June	0.336	0.01	0.03	0.11
July	0.359	0.00	0.00	0.00
August	0.347	0.00	0.01	0.04
September	0.269	0.00	0.01	0.06
October	0.199	1.20	2.90	11.23
November	0.144	1.64	4.81	19.31
December	0.089	1.16	2.24	8.06

is then used to compute the position of each CP at each given time step depending on its prior location, velocity, and acceleration in the search space (Asadieh and Afshar, 2019). Each CP has a radius of 'a' and a uniform charge density (q_i) as shown in Eq. 2:

$$q_i = \frac{fit(i) - fitworst}{fitbest - fitworst}, i = 1, 2, \ldots, N \tag{2}$$

This equation updates the variable (q_i) based on the fitness of the (i) th solution relative to the best and worst solutions in the population and N being the total number of CPs This normalization aids in making fitness values comparable and influences the selection process in optimization algorithms. The initial positions of the CPs are randomly allocated within the problem's specified limits in the search space. Meanwhile, the initial velocities of the CPs are set to zero.

The CPs are distributed throughout the exploration area and have the capability of exerting electric forces on one another. The magnitude of the force acting on a CP located inside or outside of the sphere is computed in a distinct manner. The electric force acting on the CPs inside or outside of the sphere is obtained by applying Eq. (3) (Kaveh and Talatahari, 2010).

$$F_j = q_j \sum_{i,i \neq j} \left(\frac{q_i}{a^3} r_{ij} i_1 + \frac{q_i}{r_{ij}^2} i_2 \right) p_{ij} (X_i - X_j) \begin{cases} j = 1, 2, \ldots, N \\ i_1 = 1, i_2 = 0 \leftrightarrow r_{ij} < a \\ i_1 = 0, i_2 = 1 \leftrightarrow r_{ij} \geq a \end{cases} \tag{3}$$

Where *rij* denotes the distance of separation between two particles, and F_j represents the resultant force acting on the *jth* CP.

$$r_{ij} = \frac{\left\| X_i - X_j \right\|}{\left\| \frac{(X_i + X_j)}{2} - X_{best} \right\| + \varepsilon} \tag{4}$$

Eq. (4) represents the probability of moving each CP towards the others, where X_i and X_j indicate the positions of the ith and jth CPs, respectively. X_{best} represents the position of the current best CP, while ε is a small positive value utilized to avoid singularity. The value of p_{ij} is determined by the Eq. (5).

$$p_{ij} = \begin{cases} 1 \frac{fit(i) - fitbest}{fit(j) - fit(i)} > randor \quad fit(j) > fit(i) \\ 0 otherwise \end{cases} \tag{5}$$

According to Eq. (3), the force exerted on a CP positioned inside the

sphere is directly proportional to the distance between CP. Conversely, if the CPs are located outside the sphere, the force acting between them is inversely proportional to the square of the distance between them. After computing the resultant forces acting on the CPs, their new positions are determined using the laws of motion. To achieve this, each CP goes towards its new position considering the resultant forces and its previous velocity, as indicated in Eqs. (6) and (7) (Asadieh and Afshar, 2019).

$$X_{j,new} = rand_{j1}.K_a.\frac{F_j}{m_j}.\Delta t^2 + rand_{j2}.k_v.V_{j,old}.\Delta t + X_{j,old} \quad (6)$$

$$V_{j,new} = \frac{X_{j,new} - X_{j,old}}{\Delta t} \quad (7)$$

Eq. (8) presents the acceleration coefficient K_a and the velocity coefficient K_v, which influence the motion of the CPs. The two random numbers, $rand_{j,1}$ and $rand_{j,2}$, are uniformly distributed within the interval (0,1). The mass of the *jth* CP m_j, is set equal to q_j. The time step, Δt, is set to 1. The velocity coefficient can either remain constant or change in the upcoming time steps.

$$K_a = \alpha * \left(1 + \frac{iter}{iter_{\max}}\right), K_v = \beta * \left(1 - \frac{iter}{iter_{\max}}\right) \quad (8)$$

Eq. (9) includes the current iteration number (*iter*), and the maximum number of iterations ($iter_{\max}$), set for the algorithm run. This equation establishes a linear relationship between the velocity coefficient, K_v and the acceleration coefficient, K_a, as the number of iterations increases. Specifically, K_v decreases linearly to zero, while K_a increases to 2α, which maintains a balance between exploration and convergence speed. It's worth noting that the parameters α and β in Eq. (8) are adjustable, and their values determine the acceleration and velocity coefficients (K_a and K_v). The recommended value for both α and β parameters is 0.5, as per the reference paper of the CSS algorithm. By substituting the values of K_a and K_v from Eqs. (6) to (8), Eq. (9) can be rewritten (Asadieh and Afshar, 2019).

$$X_{j,new} = \propto * rand_{j1}\left(1 + \frac{iter}{iter_{\max}}\right).\sum_{i,i\neq j}\left(\frac{q_i}{a^3}r_{ij}i_1 + \frac{q_i}{r_{ij}^2} \quad i_2\right) \quad p_{ij}(X_i - X_i)$$

$$+\beta * rand_{j2}\left(1 - \frac{iter}{iter_{\max}}\right).V_{j,old} + X_{j,old} \quad (9)$$

$$V_{j,new} = X_{j,new} - X_{j,old} \quad (10)$$

To improve the algorithm's performance, it is advisable to incorporate a memory mechanism called the Charged Memory (CM) to store the best results. If any CP moves outside the search space, it can be corrected using a harmony search-based handling approach. This involves generating or selecting a new value from the CM on a probabilistic basis.

We initialized the algorithm with the number of CPs 100 and 192 decision variables, executing 5000 iterations. The charged memory had a capacity of 5, with a sphere radius of $1 * 10^{-9}$. Algorithmic coefficients, set at 0.5 for acceleration and velocity, balanced exploration and exploitation. Boundary constraints ranged from 0 to 2.46. These parameters were fine-tuned through a rigorous procedure to optimize the algorithm's performance for our cast study.

The selection of an algorithm is a crucial decision. CSS's advantages lie in its ability to mimic the charged particles' behaviour in a dynamic system, allowing for efficient solution space exploration. The CSS algorithm's unique features, such as its adaptability and capacity for global optimization, make it well-suited for reservoir operation studies.

The primary goal of this research is not only to discover the importance of different algorithms in optimizing the operation of the reservoirs; this has been proven in various research, while the goal was to experiment with optimizing the operation of this type of rainfall-based reservoirs using one of the algorithms whose effectiveness in optimizing reservoirs has been explored before and studying the effect of sediments, on the operation of reservoirs. Other algorithms can be used, such as genetic algorithms and the PSO algorithm,. etc, to optimize this type of reservoir, and the same results may appear, but to varying degrees. This may be studied in other research to observe the effect of the difference in using different algorithms to optimize this type of reservoir.

The CSS algorithm has demonstrated noteworthy performance through rigorous testing with benchmark problems involving highly non-linear constrained and/or unconstrained real-valued mathematical models, exemplified by challenges like Ackley's function and the Fletcher–Powell function in previous research. Its efficacy in optimizing reservoir operation has been further substantiated through validation processes, encompassing convergence criteria and sensitivity analysis to ensure reliability (Asadieh and Afshar, 2019). Moreover, in this study, the algorithm has been adeptly fine-tuned to enhance result accuracy. The collective evidence underscores the CSS algorithm as a robust and applications in water resource management.

2.9. Problem formulations and constraint

The optimization of the operating problem in a reservoir is achieved by utilizing the CSS algorithm, which involves defining the objective function and identifying decision variables, system limits, and their classifications. The objective function is evaluated while staying within the limits of the constraints for the selected decision variables, and the updated set of decision variable values is determined based on the feedback assessment. The previous steps are iterated until the desired performance objective is achieved or the stopping criterion is reached. Finally, the decision-making memory process stores the selection of optimal solutions for the optimal decision variables (Gong et al., 2020).

In this research, the objective function of it is to minimize the monthly water deficit, which is represented by reducing the difference between the water released and the water demand for the reservoir in each operating period, whether it is for domestic, irrigation, or industrial purposes in (MCM/year), which can be expressed by the following Eq. (11).

$$Min \quad Z = \sum_{t=1}^{NT}\left(\frac{D_t - R_t}{D_{\max}}\right)^2 \quad (11)$$

Where D_t is water demand during operating period t, NT is the total operating period, R_t is water released during operating period t.

The water balance continuity equation can be expressed by Eq. (12), where the storage for the next period depends on the previous storage of the reservoir, Inflow, water released, water losses, and overflow from the reservoir in period t.

$$S_{t+1} = S_t + I_t - R_t - L_t - O_t \quad (12)$$

Where S_{t+1} and S_t are the final and initial reservoir storage for time t, I_t is the inflow in the reservoir, R_t is water released from the reservoir, L_t is water losses (Evaporation and seepage), and O_t is overflow from the reservoir.

Where the evaporation losses in the Mujib reservoir were calculated using Eqs. (13) and (14).

$$E_t = ER_t * \frac{A_t}{1000} \quad (13)$$

$$A_\tau = a + b * S_t + c * S_t^2 + d * S_t^3 \quad (14)$$

Where evaporation loss E_τ estimated using the average evaporation rate (ER_τ) during the time step t and surface area (A_τ) in km^2 for the reservoir as shown in Eq. (14), where surface area (A_τ) calculated by fitting equation to existing data to find relationship between surface area and storage of the reservoir, the constants a, b, c, and d are found by fitting Eq. (14).

In addition to the storage and release Constraints of the reservoir,

where the storage level is controlled at any period by controlled the storage within the maximum storage limit and the minimum storage limit as shown in Eq. (15).

$$Storage \quad Capacity = 3.774 \times 10^6 \quad m^3 \leq S_t \leq 31.232 \times 10^6 \quad m^3 \tag{15}$$

The water released within the maximum release and minimum release of the reservoir for every month as shown in Eq. (16):

$0 \leq R_t \leq R_{\max}$ (16).

where R_t Is Water released in every month and not exceed the water demand in period t.

MATLAB version R2018b by Math Work was used to optimize operation in the reservoir, where the objective function had adjusted them to fit Mujib reservoir case. Considering the monthly releases as the decision variable that the algorithm is supposed to optimize, in addition to specifying the constraint on storage and release in the programming code. And using the monthly inflow and water losses represented by the monthly evaporation and seepage values as input data for analysis. The model is tested, and parameters are set for the algorithms, and then the release is applied to the actual inflow and water losses in Mujib reservoir using operation as shown in Eq. (17).

$$Storage_{t+1} = Storage_t + Inflow_t - Losses_t - Optimum \quad Release \tag{17}$$

The storage is adjusted every month so that if the storage in any month is more than 31.232 MCM, then the storage for the next month will be kept at 31.232 MCM, but if the final storage is less than 3.774 MCM, it will not be allowed to release the next month. The reservoir release was simulated with the inflow from January 2004 to December 2019. Fig. 3 shows the steps for using the CSS algorithm to optimize reservoirs.

2.9.1. The performance indicators

The use of sequential historical data was typically required for performance testing of hydrological models (like rainfall, inflow, reservoir level). After receiving the simulation's results, the system's success or failure was assessed from many aspects. The performance indicators are used to determine if a simulation model of a reservoir system is successful or not, as well as to compare the performance of various algorithms. The reliability, resiliency, and vulnerability indicators are three common performance indicators in water resources management, which are used in most research.

Reliability index.

Reliability is a critical performance metric for optimization models, which refers to the number of instances that the release decision can fulfill demand during the simulation period. The reservoir simulation is considered better as the system's reliability index increases. Wurbs (1996) provides the concept of volumetric (R_v) as Eq. (18) (Hossain et al., 2018).

$$R_v = \frac{\gamma}{V} * 100\% \tag{18}$$

Where γ is the volume of released water and V is the volume of demand water, so the ratio between these two gives the idea of a water deficit.

The shortage index (SI) is another method for describing a model's reliability (SI). According to Wurbs (1996), the ratio of the total volume of the shortage during the year (for monthly simulation) to the total volume of the demand water can be used to indicate the shortage for each year of a simulation (Hossain et al., 2018) as shown in Eq. (19).

$$SI = \left(\frac{100}{t}\right) \sum_{T=1}^{N} \left(\frac{Water \quad deficit}{demand \quad water}\right)^2 \tag{19}$$

T= total considered time (in year).

Resiliency.

The concept of resiliency refers to the ability of a system to recover from failure in meeting the demand. It is essentially the likelihood of the reservoir system recovering from a shortfall or an unacceptable value

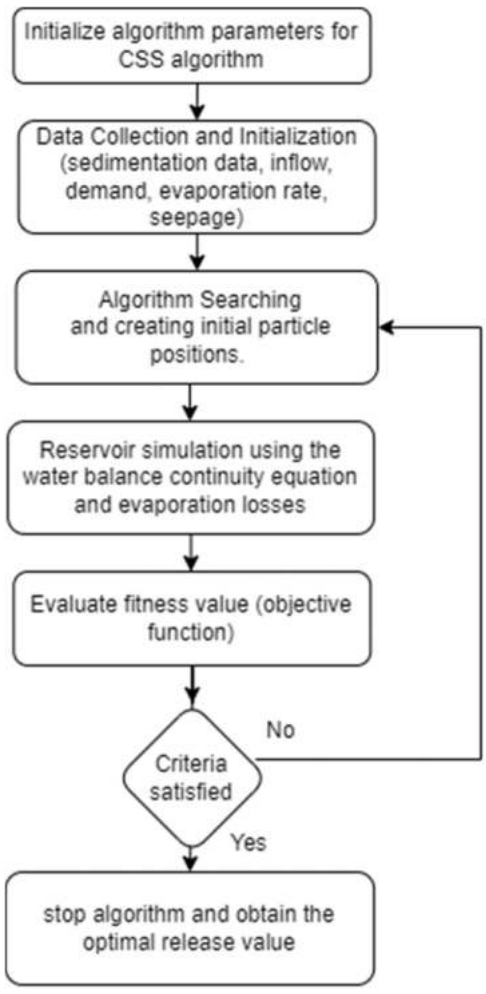

Fig. 3. The flowchart for using CSS in optimize water reservoir.

over time. A high Resiliency indicates that the reservoir has the capacity to recover and meet the demand efficiently even under unfavourable conditions, and it can be expressed using Eq. (20).

Loucks and Beek (2005) used the ratio of the total number of unsatisfactory occurrences to the number of satisfied releases that follow an unsatisfied value and total number of water shortage to calculate the resilience (Loucks and van Beek, 2017).

$$Resiliency = \frac{The \ number \ of \ times \ a \ suitable \ value \ appears \ after \ a \ shortage}{Total \ number \ of \ shortage \ periods} \tag{20}$$

vulnerability.

The reservoir system's worst-case scenario is measured by vulnerability, which is defined as a measure of the system's failure. The vulnerability index is used to assess the failure of a reservoir system model, and a lower vulnerability index value indicates a stronger system. The measure of vulnerability can be expressed mathematically, as shown in Eq. (21):

$$Vulnerability = \frac{The \ total \ of \ positive \ values \ of (Demand - Release)}{Number \ of \ times \ an \ unsatisfactory \ event \ occurred} \tag{21}$$

The proposed scenario was assessed based on error indices, such as the mean absolute error (MAE), the root mean square error (RMSE), and the correlation coefficient (R^2) for further investigation. The linear relationship between the water released and the water demand is examined using the R^2, R^2 is estimated by dividing the variance between

the water demand and the water released by the sum of their respective standard deviations. This indicator represents the difference between the water released and the water demand and demonstrates the accuracy of the linear fit, The $R^2$is calculated as shown Eq. (23). RMSE used to measure the difference between the observed values of the required variable (water demand) and the values (water released) from the model. The RMSE combines the various variances into a single measurement of the gap between the water demand and the released water, RMSE is calculated as shown Eq. (22) (Azamathulla, 2012). The MAE was considered to evaluate how the model's operation rules of the model (water released) biased by the system's demands while considering the shortage and the release excess, The MAE index is calculated as shown Eq. (24) (Yaseen et al., 2019)

$$\mathrm{RMSE} = \sqrt{\sum_{t=1}^{T} \frac{(D_t - R_t)^2}{T}} \tag{22}$$

$$R^2 = \left[\frac{\sum_{i=1}^{n} (D_t - \overline{D}_t)(R_t - \overline{R}_t)}{\sqrt{\sum_{i=1}^{n} (D_t - \overline{D}_t)^2 (R_t - \overline{R}_t)^2}} \right]^2 \tag{23}$$

$$MAE = \sum\nolimits_{t=1}^{T} \frac{|D_t - R_t|}{T} \tag{24}$$

where Dt is the water demand, Rt is the water release, T is the total number of periods of operation,

2.9.2. Scenarios

The CSS algorithm was used to optimize the operation in the reservoir under different scenarios and compare the results with the current operation without using the algorithm. Initially, the operation of the reservoir was optimized in the current operational status of the reservoir, considering the problem of sediment in the reservoir, which constitutes 20% of the volume of the reservoir. These sediments affect the actual capacity of the reservoir and its efficiency in storage water, in addition to developing a scenario with removing sediment from the reservoir.

2.9.2.1. The impact of water demand management on reservoir operation. The water demand from the reservoir is divided into domestic, agricultural, or industrial. As for the use of the reservoir water for agricultural purposes, it feeds the various agricultural lands around it from it water in seasons dedicated to agriculture, approximately 5 MCM.

Therefore, the water deficit was studied in the event that part of the demand water was not supplied from the reservoir for agricultural purposes, in the event that another source was found that feeds these agricultural crops, or the treated water was resorted to be used instead of the reservoir water for agricultural under the instructions and periodic checks by the competent authorities (Al-Mubaidin et al., 2022), or modern agricultural techniques were used that save a large part of the water used for agriculture or the use of crops that do not depend on water in abundance and can be replaced by crops that depend on small amounts of water or use water harvesting techniques and rationing citizens on them to reduce pressure on the reservoir water.

Therefore, it was imposed to reduce the demand for water by a percentage of the water allocated for agricultural purposes, and in the months that are the agricultural seasons in the cultivated lands from the water of the reservoir. It was also assumed that the demand for water would increase in the future by the amount of water that was reduced from the demand water and in the same months that the required water was reduced to notice the difference between the two cases. Therefore, the water demand from the reservoir has been modified to observe the extent of this impact on the water deficit and to help decision-makers to study the options available to them in the operation and management of the reservoir.

2.9.2.2. Effect of reservoir capacity on reservoir operation. To solve the problem of the water deficit, a suggestion to increase the storage capacity of the reservoir by different percentages of 10%, 20%, and 30% were studied by raising the dam within its possible heights to note the effect of increasing the capacity of the reservoir on reducing the water deficit. Which increases the storage capacity of the reservoir. It is one of the solutions suggested by the Jordan Water Authority to get rid of the water deficit in the reservoir and make the most of the water resulting from rainfall. It was applied to one of the neighbouring dams. In the area where Fig. 4 shows the relationship of the height of the dam with the storage capacity of the dam, where the highest storage level of the dam is 194 m, which makes the storage capacity at 31.233 MCM, and the distance at the highest storage level is at for the dam and end of the Spillway is approximately 4 m, which means the possibility of increasing the height of the dam to increase the capacity future storage reservoir.

The operation of the reservoir has been optimized without regard to the sediment problem that the reservoir faces in the current situation, to note the effect of increasing the volume of the reservoir on the problem of water deficit in general. It was suggested to increase the storage capacity of the reservoir by different percentages.

2.9.2.3. Effect of reservoir capacity with decreasing demand on reservoir operation. It was suggested to optimize the reservoir using CSS algorithms in the case of removing sediment and managing the demand water by trying to reduce it as previously mentioned and increase the storage capacity of the reservoir to observe the water deficit values when these cases are combined with each other.

The results were compared in terms of reaching the objective function using the CSS algorithm, which is to reduce the annual water deficit in the reservoir for all scenarios. In addition to simulating the release resulting from the CSS algorithm and the water demand to note the difference between the release and the demand for water in each scenario and simulating the change in the storage values of the reservoir from the CSS algorithm compared to the actual water flow of the reservoir for each scenario in addition to the annual water deficit values from the CSS algorithm for each scenario. Risk analysis (volumetric reliability, shortage index (SI), resilience, vulnerability) and error evaluation indexes (R^2, RMSE, and MAE) were used to compare results between scenarios. These results aim to present the different scenarios to the decision makers to search for their results to try to solve the water shortage problems before they occur in the future and inform them of the impact of sediment in the reservoir and try to solve it in this reservoir and avoid its formation in future reservoirs.

3. Result and discussion

3.1. Sedimentation calculation

3.1.1. Model calibration

The study's primary goal is to determine monthly sedimentation values and the cumulative sedimentation impact on the Mujib dam. This investigation also seeks to evaluate the effect of sedimentation on the dam's maximum volume by incorporating it into the dam simulation. Unfortunately, the available data for sedimentation affecting the Mujib dam is limited to four discrete measurements obtained using the Eco-Sounder device at intervals spanning from 2003 to 2015 (specifically, during the periods 2003–2005, 2006–2008, 2009, and 2010–2015), as detailed in Table 2.

Given this scarcity of data, a calibration process is undertaken, wherein surface runoff and peak runoff are considered. The physical factors described in Eq. (1) were getting (soil erodibility factor, coarse fragment factor, the support practice factor, and the slope length factor).

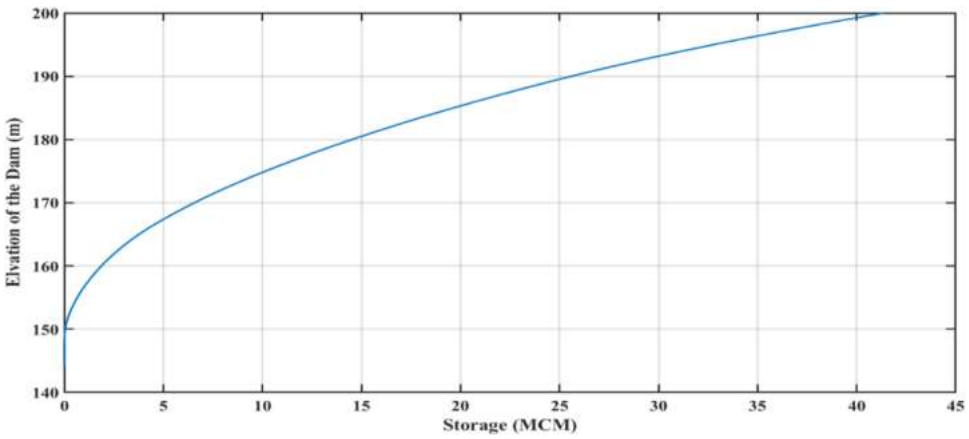

Fig. 4. The relationship between the height of the dam and the storage capacity of the reservoir.

Table 2
Accumulated observed data by Eco-sounder device.

Year	Observed data by Eco-Sounder device (m^3)
2003-2005	917,823
2006-2008	523,087
2009	510,166
2010-2015	1608,008

The cover and management factor (C) is retained for calibration with the cumulative sedimentation volume measured in the reservoir over the four specified periods. The calculated sediment is divided by 1.3, assuming an average weight of 1.3 tons/m^3 for the sediment unit.

Upon completion of the calibration process, the optimal C value is determined to be 0.00779, resulting in the lowest error compared to the measured values. The correlation coefficient (R^2) is found to be 0.982, and the model efficiency E_{model} is calculated as 0.9147. Subsequently, simulated sediments for the observed sediment period are computed, and the relationship between measured and simulated sediments is visually represented in Fig. 6.

Fig. 5 provides a clear depiction of the strong relationship between the measured and simulated sediments, affirming the efficacy of the calibration process and the chosen C value in accurately representing sedimentation dynamics in the Mujib dam. These findings contribute to a comprehensive understanding of the sedimentation patterns and their implications for the dam's volume, thereby enhancing the reliability of the dam simulation model.

Due to the limited readings of cumulative sediment readings of the Mujib dam, the cumulative sediment yield measured according to the volume of inflow in each year was redistributed as a percentage of the total inflow during the sediment measurements period as shown in Table 3.

But what concerns us is the quantities of monthly sediments that we use in simulating the reservoir, the simulated sediment obtained from applying the MUSLE model from the beginning of 2004 to the end of 2019, where the accumulated sediments at the end of 2019 was 4552,122 m^3, which represents a decrease of 14.6%. Using the linear regression method for the accumulated sediment results shown in the following table results in the regression line in Fig. 6 and the resulting slope.

Using these readings, we can predict the size of the accumulated sediments for the years 2030 2040 2050. The accumulated sediments in the reservoir will be 7492,692 m3, 10,180,811 m3, 12,868,931 m3, respectively. This result represents reduction in reservoir storage capacity 23.99%, 32.60%, and 41.20%, for the years 2030, 2040, and 2050 respectively.

Fig. 7 shows the impact of the storage capacity of the reservoir by the accumulation of sediment in the reservoir over time, as the storage capacity was 31.233 MCM at the beginning of the operation of the reservoir in 2003 and with the accumulation of sediment, the storage capacity reached 26.68 MCM at the end of 2019, which led to a decrease in storage capacity by 14.6% of its volume, which increases problems reservoir and effect on the reservoir for performing its work properly.

The aim of all this is to simulate the monthly sediment values to be

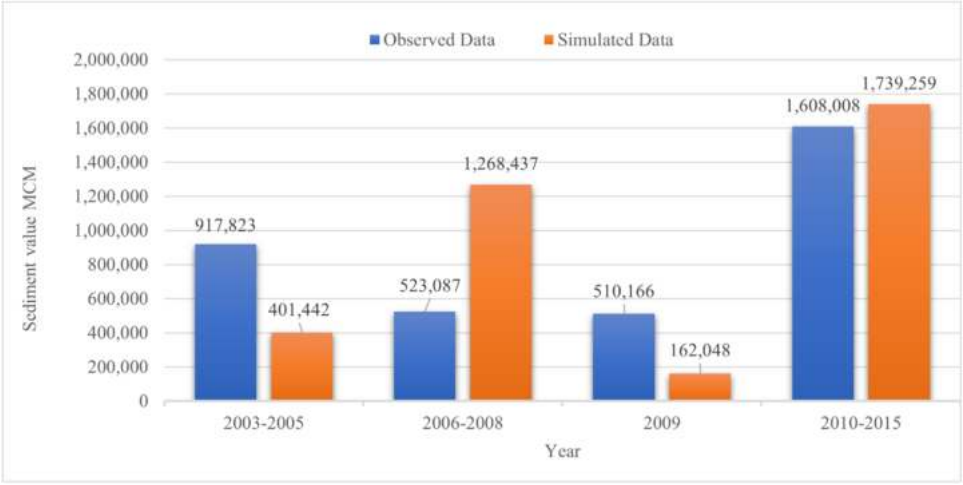

Fig. 5. Comparison of the Simulated Data for the Calibrated Period with the Observed Data.

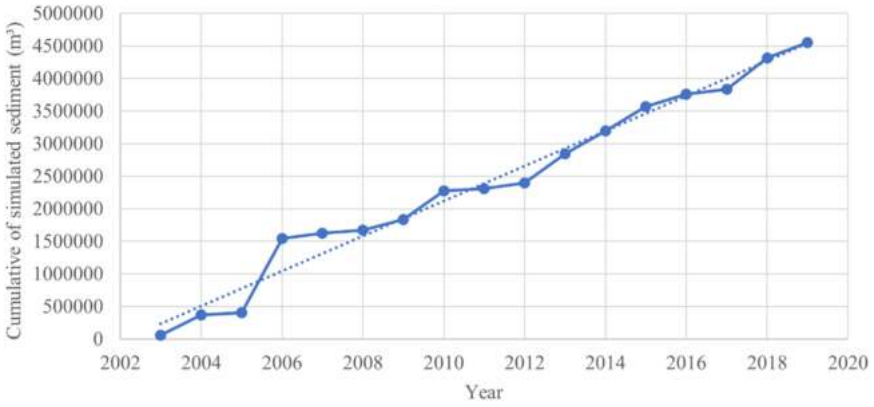

Fig. 6. Regression Line for the Cumulative of Simulated Sediment for the Years 2003- 2019.

Table 3
Distribution of sediment yields based on annual inflow.

Year	Inflow water (m^3)	Percent of Inflow during the measured sediment (%)	Observed Sediment Yield (m^3)	Simulated sediment yield (m^3)	Observed data by Eco-Sounder device (m3)
2003	5728,340	16%	148,607	57,819	917,823
2004	26,563,815	75%	689,128	315,836	
2005	3,087,143	9%	80,088	28,589	523,087
2006	73,151,767	86%	448,781	1140,875	
2007	7538,919	9%	46,251	83,499	
2008	4573,032	5%	28,055	44,212	
2009	14,713,135	100%	510,166	161,096	510,166
2010	33,251,945	23%	376,953	441,623	1608,008
2011	3641,262	3%	41,278	36,405	
2012	8508,885	6%	96,459	84,669	
2013	36,586,038	26%	414,749	448,799	
2014	28,549,370	20%	323,644	351,730	
2015	31,308,729	22%	354,924	376,033	

included in the reservoir simulation later.

3.2. Reservoir simulation results

As previously stated, this particular reservoir relies entirely on rainfall over the watershed areas, resulting in daily, monthly, and annual fluctuations in its inflow. Hence, Fig. 8 depicts the monthly inflow of water into the reservoir from its inception in 2004 until 2019. The distribution of inflow quantity into the reservoir is not uniform. The findings reveal that the reservoir does not receive significant and dependable inflow in most months of the year, and the storage of water in the reservoir is contingent on intense storms that result in high inflow, which may occur only in one or two months of the year.

On occasion, the monthly or total inflow into the reservoir surpasses

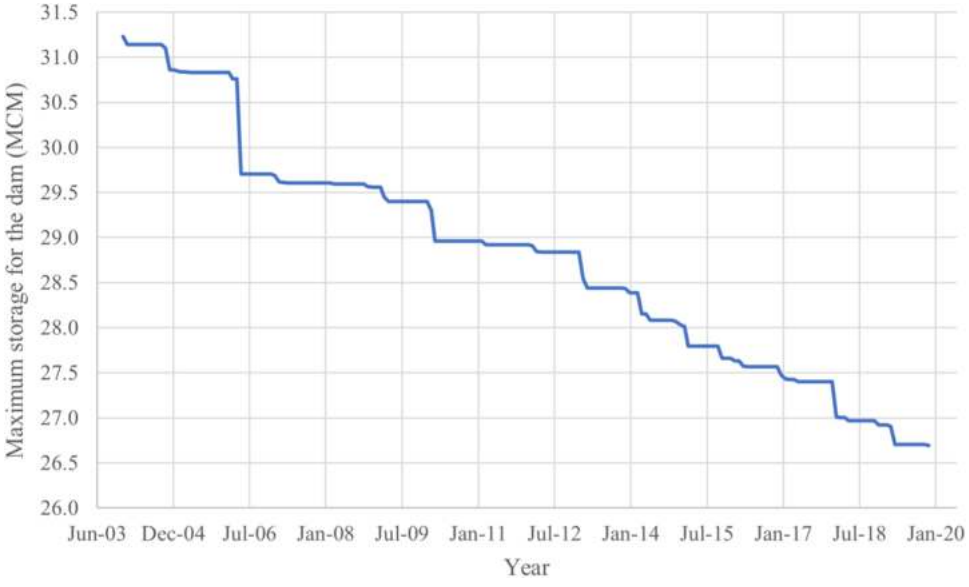

Fig. 7. The effect of sedimentation on the decrease in the actual maximum volume of the reservoir.

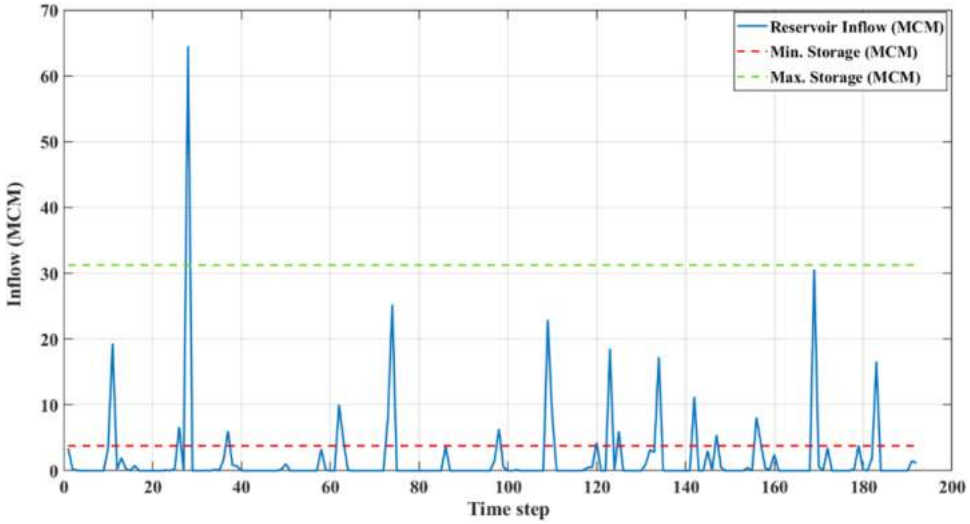

Fig. 8. The observed inflow of Mujib reservoir (MCM).

its maximum storage capacity, resulting in flooding above the dam. These significant inflows occur only once or twice a year and are challenging to anticipate due to the unpredictable nature of climate changes in the region.

Table 1 reveals that the average monthly inflow into the reservoir during the last three months of the year (December, November, and October) is significantly lower than the average monthly inflow during the first four months of the year (April, March, February, and January). Moreover, rainfall during these months is not always guaranteed, and from May to September, the inflow into the reservoir comes to a halt due to the absence of rainfall in the region after the winter season.

The operational performance of the reservoir was simulated using historical data, including water demand, inflow, and water losses (such as seepage and evaporation). The extent of evaporation loss ($E_{v,\tau}$) is directly proportional to the surface area of the reservoir ($A_{v,\tau}$). The value of $E_{v,\tau}$ is calculated using the relationship between the surface area of the reservoir and the monthly average evaporation rates, which is expressed by Eq. (13). Additionally, the surface area of the reservoir during a given month $A_{v,\tau}$ depends on the storage of water in the reservoir during that period, as shown in Eq. (25).

$$A_{v,\tau} = 0.10116 + 0.10136 * S_{v,\tau} + 3.43 * 10^{-3} * {S_{v,\tau}}^2 + 5.226 * 10^{-5} * {S_{v,\tau}}^3 \quad (25)$$

Where $A_{v,\tau}$ represents the surface area for the dam during the month τ in km^2, $S_{v,\tau}$ represents the storage volume of the reservoir during the month τ in MCM.

3.3. Optimizing reservoir operation with CSS algorithm

3.3.1. Current operation with sediment effect

The water demand and the actual release of the current operation of the reservoir were simulated, as shown in Fig. 9.a, considering the existence of a problem of sediment formation accumulated in the dam during the operational period of the reservoir (192 months) after simulating the volume of monthly sediment accumulated in the dam, which works to reduce the actual volume of the reservoir.

The problem of water deficit increases with the increase in sediment accumulation and the lack of solutions to remove it, which may constitute a real obstacle to benefiting from the reservoir as required, it represents constant monthly water demand values throughout the operating years and variable released water that depends on the inflow to the reservoir and the water volume in the reservoir, considering the variable evaporation losses that depend on the water volume in the reservoir and the water loss values from the seepage, the average seepage value in a month formed during the operational periods of the reservoir is approximately 0.065 MCM.

The reservoir exhibits two distinct operating phases, with the demarcation point at the onset of 2013. The pre-2013 phase faced considerable water deficits attributed to insufficient inflow values during the reservoir's initial operational stages, rendering it unable to meet demand. Subsequently, the reservoir encountered multiple drought periods, leading to an irregular release of water and an inadequate supply. Looking ahead, there is a pressing need to develop operational plans that account for the reservoir's historical performance, inflow variations, and current storage. Algorithms can play a crucial role in optimizing future reservoir operations, minimizing potential water deficits, and ensuring sustainable water supply.

The CSS algorithm was used to optimize the operation of the Mujib reservoir by using monthly reservoir inflow data over 16 years, from 2004 to 2019 (192 monthly periods), and considering release water as decision variables. Table 4 shows the general characteristics of the Mujib reservoir. The parameters of the CSS algorithm mentioned in Table 5, which were adjusted and tested, were used to obtain the best results in optimizing the operation of the reservoir using the CSS algorithm.

Table 6 shows the results of 10 runs of the algorithm for the objective function and their statistical values, considering the amounts of accumulated sediment and the values of water losses from evaporation and seepage. The best result for the objective function is 12.163. The results showed that the standard deviation of the objective function values is close to zero, indicating that all 10 runs converge to almost one single solution.

The convergence curve is a critical indicator illustrating the optimization algorithm's efficacy in reaching the optimal solution over successive iterations. It serves as a measure of the algorithm's speed in achieving the objective function, primarily cantered around minimizing the square deficit. In Fig. 11.a, the convergence curve of the CSS algorithm is depicted, showcasing its performance in optimizing the Mujib reservoir's operation amid sediment-related challenges. Notably, the algorithm reached the minimum fitness point within 1500 iterations, underscoring its efficiency in addressing the reservoir's complexities.

Fig. 9.b shows the best solution obtained by the CSS algorithm in terms of the monthly released water during the operation period of the reservoir (192 months) versus the monthly demand water, considering the problem of sediment and water losses in terms of evaporation and seepage. Fig. 9.b illustrates a notable reduction in drought periods achieved through the utilization of CSS algorithms compared to the operational mode without their application. The CSS algorithms

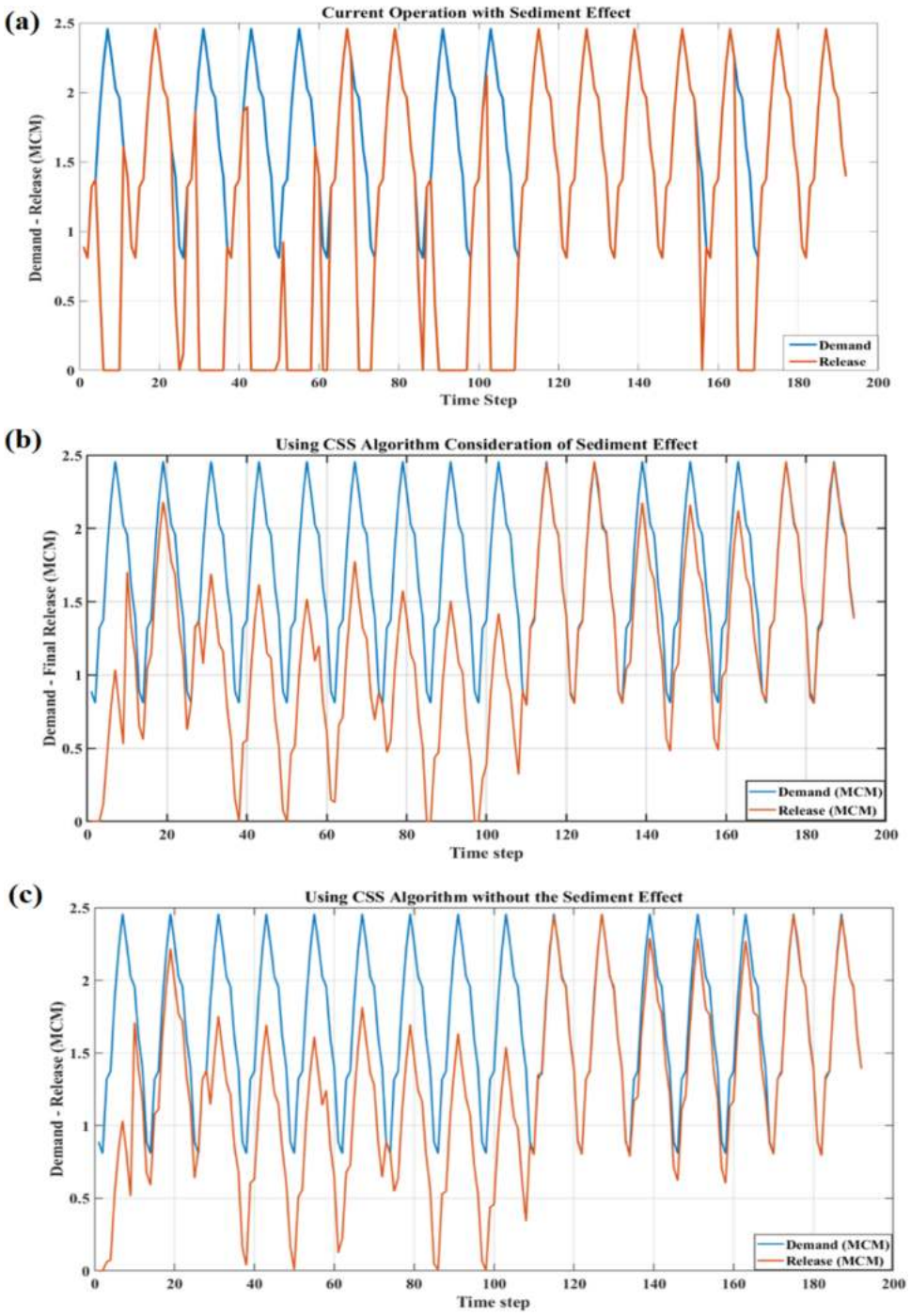

Fig. 9. Water demand and released water for Mujib reservoir (a) current operation with sediment effect (b) using the CSS algorithm with sediment effect (c) using the CSS algorithm without sediment effect.

Table 4
General characteristics of the Mujib reservoir.

Reservoir parameters	Value (MCM)
Storage capacity for the reservoir	27.46
Initial storage for the reservoir	5.73
The average annual reservoir inflow	22.24
Annual water demand	20.16
Minimum allowable storage volume	3.77
Maximum allowable storage volume	31.23
Maximum water release (Max. Demand)	2.46
Minimum water release	0.00

Table 5
The parameters of the CSS algorithm.

Parameter	Value
Number of CPs	100
Number of Decision Variables	192
Number of iterations	5000
Capacity of Charged Memory (CM)	5
Radius of charged spheres	$1 * 10^9$
Acceleration Coefficient	0.5
Velocity Coefficient	0.5

Table 6
Ten random results for the reservoir system in optimal operation using CSS algorithm under different scenarios.

Run	with Sedimentation	without Sedimentation	Decreasing Demand	Increasing Demand	Increase Storage 10%	Increase Storage 20%	Increase Storage 30%	Increase storage 10% with decreasing demand	Increase storage 20% with decreasing demand	Increase storage 30% with decreasing demand
1	12.941	10.996	7.036	16.440	9.468	8.558	8.054	5.933	5.229	4.876
2	12.935	10.997	7.040	16.439	9.463	8.550	8.048	5.935	5.229	4.875
3	12.935	10.991	7.036	16.444	9.459	8.551	8.049	5.936	5.230	4.876
4	12.940	10.995	7.040	16.444	9.460	8.555	8.047	5.938	5.226	4.876
5	12.940	10.991	7.035	16.441	9.465	8.550	8.052	5.936	5.231	4.876
6	12.937	10.992	7.044	16.441	9.468	8.558	8.054	5.933	5.229	4.876
7	12.940	10.998	7.036	16.433	9.463	8.550	8.048	5.935	5.229	4.875
8	12.937	10.996	7.034	16.442	9.459	8.551	8.049	5.936	5.230	4.876
9	12.935	10.999	7.035	16.439	9.460	8.555	8.047	5.938	5.226	4.876
10	12.941	10.996	7.040	16.443	9.465	8.550	8.052	5.936	5.231	4.876
Best Solution	12.935	10.991	7.034	16.433	9.459	8.550	8.047	5.933	5.226	4.875
Worst Solution	12.941	10.999	7.044	16.444	9.468	8.558	8.054	5.938	5.231	4.876
Average of Solutions	12.938	10.995	7.038	16.441	9.463	8.553	8.050	5.935	5.229	4.876
Standard Deviation	0.0026	0.0028	0.0031	0.0032	0.0036	0.0035	0.0029	0.0016	0.0020	0.0005

contribute by supplying released water strategically to minimize water deficit values and mitigate prolonged drought periods within the reservoir. This approach ensures a consistent supply of water, even if it doesn't fully meet the total demand, by reducing released water by a small percentage before anticipated drought periods. The objective is to secure water supply after these periods, thereby minimizing drought occurrences in situations of insufficient water inflow. Release curves closely aligned with demand facilitate achieving a minimal water deficit, emphasizing the effectiveness of the CSS algorithms in reservoir management.

Fig. 10.a visually depicts the storage volume values at each time step, constrained within the maximum and minimum allowable storage limits, considering the historical inflow of the reservoir. The stability of the maximum allowable storage limit is evident, showcasing the reservoir's consistent upper capacity. However, noteworthy changes are observed in the minimum allowable storage limit due to sediment accumulation in the dam over time. This necessitates adjustments to accurately simulate the reservoir's state, reflecting the reduction in actual storage volume caused by sediment buildup. The increase in sediment volume exacerbates the water deficit issue, emphasizing the importance of sediment removal to maintain reservoir functionality.

Fig. 10.a illustrates the dynamic changes in reservoir storage volume over time, influenced by the varying inflow patterns. Periods of declining storage are noticeable, indicating instances when the reservoir is utilized to supply water demand while accommodating the incoming water from rainfall during specific months. Additionally, the figure highlights periods where the storage volume approaches zero, signifying continuous water release without sufficient inflow to replenish the deficit. This scenario poses a challenge for the reservoir in meeting water demand. The allowable storage limit is defined by Eq. (26), guiding the reservoir's operational constraints.

$$S \quad \min_{t+1} = S \quad \min_t + Sed_t \tag{26}$$

Where $S_{\min}$ represents the minimum allowable water storage which increases with the accumulation of sediment in the dam and sed_t represents the sedimentation values formed over the time.

The minimum allowable water storage at the end of the dam's operational period in 2019 reached 8.32 MCM instead of 3.774 MCM at the beginning of the dam's operational period in 2004.

3.3.2. Optimizing the operation of the reservoir, considering the removal of sediment from the reservoir

The operation in the reservoir has been optimized assuming that these sediments are removed from the reservoir to restore the actual storage volume of the reservoir to its normal state and compare the water deficit in both cases with the presence of sediment or not. Fig. 11.b shows the convergence curve of the CSS algorithm when it is used to optimize the operation in the Mujib reservoir in the case of removal of sediment, where the minimum fitness was reached within 1500 iterations, it's like when using algorithm in the case of sediments. The best result of the objective function between the 10 runs for the algorithm was 10.991 as shown in Table 6, which indicates the extent of the effect of sediment removal by reducing the water deficit.

Fig. 9.c shows the best solution obtained by the CSS algorithm in terms of the monthly released water during the operation period of the reservoir (192 months) versus the monthly demand water, considering the removal of the sediment and water losses in terms of evaporation and seepage.

The pattern of Fig. 10.a that includes the sedimentation amount is like the pattern in Fig. 10.b that ignores the calculation of sedimentation amount, while there is a slight difference in the numbers that will be clarified later. Fig. 10.b shows the storage volume values at each time step are confined between the maximum and minimum allowable storage with the historical inflow of the reservoir considering removal the sediment. The line that represents the volume of storge in the reservoir is

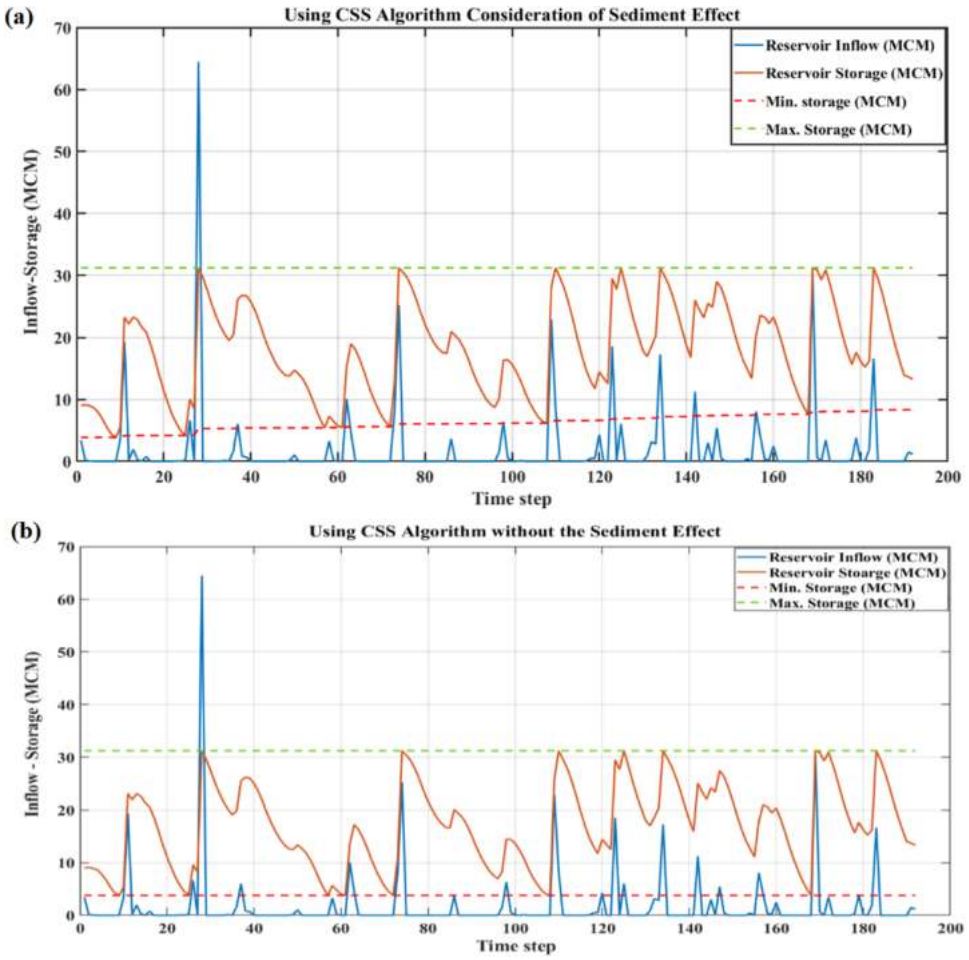

Fig. 10. Water inflow and Storage volume for Mujib reservoir using the CSS algorithm (a) with sediment effect (b) without sediment effect.

shown between the minimum allowable storage limit and the maximum allowable storage limit, with both limits remaining constant to ignore the problem of sediment formation.

Indexes serve as valuable tools for comparing the outcomes of different scenarios. The optimal system is characterized by lower RMSE and MAE values and higher R^2 values. Table 7 presents the results of error indexes for various scenarios. In the context of sediment removal using the CSS algorithm, superior values were achieved, with R^2, RMSE, and MAE at 0.58, 0.59, and 0.44, respectively. In comparison, when addressing sediment-related issues with the algorithm, the values were 0.55, 0.64, and 0.49 for R^2, RMSE, and MAE. Both scenarios outperformed the standard operational system, without algorithmic intervention and considering sediment impact, where R^2, RMSE, and MAE were notably lower at 0.10, 1.00, and 0.54, respectively.

These indexes—volumetric reliability (*Rv*), shortage index (*SI*), and resilience and vulnerability index—are instrumental in precisely comparing scenarios related to water supply for downstream demands. Optimal system performance is characterized by minimal *SI* and vulnerability index values and maximal *Rv* and resilience values. Table 8 illustrates the results of these indexes when employing the CSS algorithm for the Mujib reservoir.

The *Rv* values demonstrated notable improvement when utilizing the CSS algorithm without considering sediment in the reservoir, reaching 74.11. In comparison, the *Rv* values were 71.11 when employing the algorithm with sediment calculation. Both outperformed the *Rv* in the normal operational mode without the algorithm for sediment calculation, which stood at 67.97.

The utilization of the CSS algorithm for both optimizing operation and sediment removal resulted in the lowest possible values for *SI* and Vulnerability, recorded at 11.28 and 0.51, respectively. In comparison, when employing the CSS algorithm for optimizing reservoir operation while considering sediment calculations, the values were 13.24 for *SI* and 0.56 for Vulnerability. These values outperformed those in the normal operational mode with sediment, which stood at 19.70 for *SI* and 0.84 for Vulnerability.

The values of the resilience were as low as possible in the normal operation mode without using the CSS algorithm and calculating the sediment, where the value was 0.29 better than the values when using the algorithm in both cases when calculating the sediment and when not calculating the sediment 0.09 and 0.10 respectively. The resilience index assesses the system's ability to recover after failing to meet water demand fully. It specifically considers the months when water demand was entirely satisfied. However, it doesn't elucidate changes in the total water deficit values with algorithmic interventions, nor does it articulate the percentage of monthly demand met from the reservoir.

The continuous droughts, resulting in the reservoir being depleted, were alleviated through the utilization of the CSS algorithm. However, it comes at the cost of not fully meeting water demand in certain months. The primary aim of the CSS algorithm is to minimize the water deficit, even if it means not fully releasing water in several periods, with a slight variance from the demanded water. This strategy aims to compensate for shortages during drought periods that impact the reservoir's water levels. Hence, the CSS algorithm might extend the duration in which the released water doesn't precisely align with the demand, albeit with a minor difference. Consequently, the resilience values in the regular operation surpass those without the CSS algorithm. Nonetheless, the

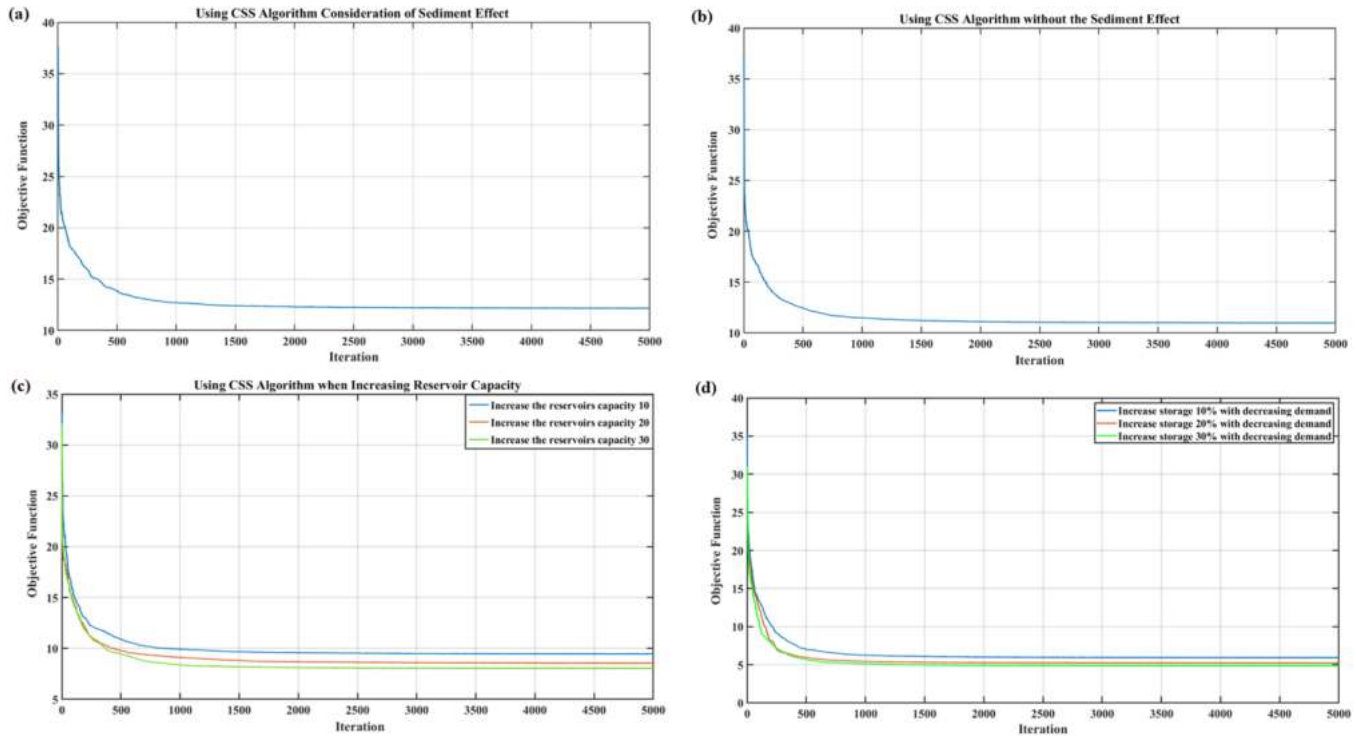

Fig. 11. Convergence curve of the optimum solution of Mujib reservoir using the CSS algorithm (a) with sediment effect (b) without sediment effect (c) considering increasing in storage capasity of the reservoir (d) considering increasing in storage capasity of the reservoir and decreasing the demand.

Table 7
Indexes result of the release curves for Mujib reservoir using CSS algorithm compared to the current operation.

Performances	Current Operation with Sediment Effect	with Sediment	without Sediment	Decreasing Demand	Increasing Demand	Increase Storage 10%	Increase Storage 20%	Increase Storage 30%	Increase storage 10% with decreasing demand	Increase storage 20% with decreasing demand	Increase storage 30% with decreasing demand
R^2	0.10	0.55	0.58	0.73	0.36	0.61	0.62	0.63	0.74	0.75	0.75
RMSE(MCM)	1.00	0.64	0.59	0.47	0.72	0.55	0.52	0.50	0.43	0.41	0.39
MAE (MCM)	0.54	0.49	0.44	0.31	0.57	0.40	0.37	0.35	0.28	0.26	0.25

Table 8
Risk analysis result of the release curves for Mujib reservoir using CSS algorithm compared to the current operation.

Performances	Current Operation with Sediment Effect	with Sediment	without Sediment	Decreasing Demand	Increasing Demand	Increase Storage 10%	Increase Storage 20%	Increase Storage 30%	Increase storage 10% with decreasing demand	Increase storage 20% with decreasing demand	Increase storage 30% with decreasing demand
Volumetric Reliability (*Rv*)	67.97	71.11	74.11	79.37	69.93	76.61	78.48	79.45	81.45	82.66	83.58
Shortage index (SI)	19.70	13.24	11.28	6.86	21.78	9.68	8.87	8.34	5.74	5.08	4.71
Resilience	0.29	0.09	0.10	0.12	0.10	0.05	0.11	0.15	0.15	0.12	0.16
Vulnerability	0.84	0.56	0.51	0.36	0.65	0.44	0.44	0.42	0.36	0.33	0.31

water distribution is optimized to minimize the water deficit, as demonstrated in Table 9.

Table 9 outlines the annual water deficit values concerning the use of the algorithm with or without sediment calculations, juxtaposed with the baseline scenario involving sediment calculations. This table serves as a crucial metric for evaluating the algorithm's efficacy in optimizing reservoir operation. The water deficit values without sediment calculations using the CSS algorithm reached an optimal low at 83.79 MCM, outperforming scenarios involving sediment calculations (93.53 MCM) and the standard operating situation with sediment calculations (103.30 MCM). This signifies that the algorithm contributed to an 18.89% reduction in water deficit with sediment removal and a 9.46% reduction with sediment calculations.

3.3.3. The impact of water demand management on reservoir operation

The impact of water demand management on reservoir operation is elucidated through the outcomes of 10 runs of the CSS algorithm, as presented in Table 6. Focused on optimizing reservoir operation under

Table 9
Annual water deficit values (MCM) of the Mujib reservoir using CSS algorithm compared to the current operation.

Year	Current Operation with Sediment Effect	with Sediment	without Sediment	Decreasing Demand	Increasing Demand	Increase Storage 10%	Increase Storage 20%	Increase Storage 30%	Increase storage 10% with decreasing demand	Increase storage 20% with decreasing demand	Increase storage 30% with decreasing demand
2004	12.14	12.27	12.05	10.15	14.00	12.03	12.08	12.08	10.15	10.12	10.13
2005	0.91	3.14	2.93	0.40	5.36	2.92	2.89	2.88	0.40	0.43	0.41
2006	15.49	6.67	6.07	4.71	7.51	5.43	4.65	4.17	3.96	3.25	2.74
2007	12.01	9.99	9.20	7.47	10.91	8.15	7.08	6.27	6.35	5.12	4.39
2008	16.16	10.25	9.60	7.21	11.97	8.60	7.77	6.85	6.37	5.55	4.79
2009	7.48	8.41	8.10	5.89	10.32	8.09	8.13	7.78	5.84	5.91	5.38
2010	0.89	8.67	7.80	6.20	9.36	7.09	7.92	7.86	5.45	5.86	5.89
2011	16.40	11.09	10.04	7.98	12.17	9.13	8.48	8.58	7.04	6.42	6.38
2012	12.68	12.01	11.15	8.74	13.53	10.11	9.46	9.42	7.76	7.02	7.03
2013	0.89	0.058	0.11	0.07	0.12	0.10	0.09	0.07	0.05	0.05	0.03
2014	0.00	0.08	0.07	0.09	0.10	0.06	0.08	0.11	0.05	0.07	0.01
2015	0.00	2.97	1.78	0.10	3.41	1.01	0.28	0.09	0.05	0.05	0.06
2016	1.60	3.74	2.33	0.17	4.43	1.32	0.37	0.12	0.06	0.05	0.02
2017	6.98	4.05	2.40	0.16	4.76	1.43	0.42	0.12	0.03	0.013	0.04
2018	0.89	0.03	0.08	0.08	0.11	0.11	0.12	0.04	0.04	0.09	0.04
2019	0.00	0.15	0.07	0.10	0.08	0.12	0.09	0.09	0.08	0.03	0.03
∑	103.30	93.53	83.79	59.52	108.11	75.71	69.90	66.53	53.67	50.06	47.38

potential variations in future water demand, the results reveal noteworthy patterns. The most favourable result for the objective function, considering a decrease in demand water, is 7.034. Conversely, in scenarios anticipating an increase in demand water, the best outcome for the objective function is 16.433. Table 7 shows the error-index values, where we notice the big difference between the values of these coefficients in the two cases, where the values of R^2, RMSE, and MAE in the case of demand water decreasing were 0.73, 0.47, and 0.31, respectively, while their values were 0.36, 0.72, and 0.56 respectively in case increasing demand.

Noting the difference between an increase in the *Rv* and a decrease in the SI and vulnerability in case of a decrease in the demand water and an increase in the demand water. Table 9 shows the values of the total water deficit of the reservoir when using the CSS algorithm to optimize the operation of Mujib reservoir in case of decreasing or increasing the demand water from the reservoir. The values of the total water deficit of the reservoir in the case of an increase in the demand water were 108.11 MCM, this increases the water deficit by 4.55%, while in the case of a decrease in the demand water was 59.51 MCM and this reduces the water deficit by 42.39%.

3.3.4. Effect of reservoir capacity on reservoir operation

Transitioning to the effect of reservoir capacity on operation, Table 6 details results from 10 runs of the CSS algorithm under varying storage capacities. The best results in the case of increasing the storage capacity by 10%, 20%, and 30% are 9.459, 8.550, and 8.047, respectively. Fig. 11.c, visually represents the convergence curves, indicating a reduction in the objective function with increased storage capacity. This aligns with expectations, showcasing the algorithm's effectiveness in mitigating water deficits. Further analysis in Table 7 explores error-index values in the context of optimizing the reservoir by the CSS algorithm in the case of increasing the capacity by 10% 20% 30%. The results of the best R2, RMSE, and MAE values were when increasing the reservoir capacity by 30%, where their values were 0.63, 0.50, and 0.35 respectively, while their values when increasing the capacity of the reservoir were 20% were 0.62, 0.52 and 0.37 respectively and their values when increasing the capacity of the reservoir 10% are 0.61, 0.55 and 0.40 respectively.

Table 8 presents the results of the risk analysis when optimizing the reservoir with the CSS algorithm, considering an increase in the reservoir's storage capacity by 10%, 20%, and 30%, while disregarding sediment-related issues. The most favourable values for Rv, SI, and Vulnerability were observed in the case of a 30% increase in storage capacity, with values of 79.45, 8.34, and 0.42, respectively. For a 20% increase in storage capacity, the values were 78.48, 8.87, and 0.44, and for a 10% increase, they were 76.61, 9.68, and 0.44, respectively. Moreover, the observed trends in risk analysis, as presented in Table 8, substantiate the advantages of augmenting reservoir storage capacity. The higher Rv values indicate enhanced reliability, while lower SI and Vulnerability values signify reduced susceptibility to adverse events. Notably, the 30% increase in storage capacity outperforms the other scenarios, underscoring the algorithm's ability to not only optimize water supply but also fortify the reservoir system against potential risks.

Table 9 shows the annual water deficit values when optimizing the reservoir using CSS algorithm when the capacity of the reservoir is increased by a percentage 10%, 20% and 30%. The total water deficit was the least possible when the reservoir capacity was increased by 30%, the deficit value was 66.53 MCM, the total water deficit in the case of increasing the capacity of the reservoir by 10% and 20% are 75,71 MCM and 69,90 MCM respectively.

The comprehensive evaluation provided in this study underscores the multifaceted benefits of reservoir capacity optimization. The synergy between the CSS algorithm's effectiveness in minimizing water deficits and its positive impact on risk metrics signifies a holistic approach to reservoir management. These findings hold significant implications for water resource planners and policymakers, suggesting that strategic investments in reservoir capacity expansion, particularly by 30%, can yield substantial improvements in both performance and resilience. Future research could delve into finer-grained analyses, considering dynamic factors such as climate variability and evolving water demand patterns, to further refine and validate these promising results.

3.3.5. Effect of reservoir capacity with decreasing demand on reservoir operation

Fig. 11.d shows the convergence curve of the CSS algorithm in the case of ignoring the sediment problem and the demand water management by trying to reduce it and increase the storage capacity of the reservoir within different percentages. The pattern of the curve was like that of the previous curves of the rate of convergence. Table 6 shows the results of the 10 runs for the CSS algorithm in this case. The better value in the case of reducing the demand water and increasing the storage capacity of the reservoir 10% 20% 30% are 4.875, 5.226, and 5.933 respectively. Table 7 shows the values of the error index when using the CSs algorithm in the case of reducing the demand water from the reservoir and increasing the storage capacity of the reservoir without regard to the sediment in the reservoir.

The values of R^2, RMSE, and MAE achieved their maximum levels when disregarding the sediment issue and optimizing the reservoir for a 30% decrease in demand water and an increase in storage capacity. Specifically, in this scenario, their values were 0.75, 0.39, and 0.25, respectively. Similarly, when overlooking the sediment problem and optimizing for a 20% reduction in demand water and increased storage capacity, these values were 0.75, 0.41, and 0.26. For the case of disregarding the sediment issue and optimizing for a 10% decrease in demand water and increased storage capacity, the values were 0.74, 0.43, and 0.28, respectively.

The outcomes of the risk analysis during the optimization of the reservoir utilizing the CSS algorithm are presented in Table 8. This analysis pertains to scenarios involving a reduction in water demand from the reservoir and an increase in the reservoir's storage capacity by 10%, 20%, and 30%, with no consideration for sedimentation. Notably, the most favourable values for *Rv*, SI, and Vulnerability are observed when increasing the storage capacity of the reservoir by 30%. Specifically, these values are 83.58, 4.71, and 0.31, respectively. Corresponding values for a 20% increase in storage capacity are 82.66, 5.08, and 0.33, while a 10% increase yields values of 81.45, 5.74, and 0.36 for *Rv*, SI, and Vulnerability, respectively. This data illustrates the influence of varying storage capacity scenarios on risk-related metrics, emphasizing the potential benefits of a substantial increase in reservoir storage capacity.

Table 9 shows the values of the total water deficit of the reservoir when using the CSS algorithm to optimize the operation of Mujib the in the case of reducing the demand water from the reservoir and increasing the storage capacity of the reservoir without regard to the sediment in the reservoir, the values of the total water deficit of the reservoir in the case of an increase storage capacity by 30%, 20%, 10% are 47.38 MCM, 50.05 MCM, and 53.67MCM respectively.

In conclusion, the study's findings underscore the effectiveness of the CSS algorithm in optimizing the Mujib reservoir's operation, particularly when addressing water demand management and storage capacity enhancement. The observed trends in convergence curves, error indices, and risk-related metrics consistently point towards the significance of substantial increases in reservoir storage capacity, showcasing a positive correlation with improved system performance. The detailed risk analysis in Table 8 provides valuable insights into the algorithm's ability to minimize vulnerability and enhance system resilience under various scenarios. Furthermore, the reduction in total water deficit demonstrated in Table 9 reaffirms the algorithm's potential for practical impact in alleviating water scarcity concerns. These results not only contribute to the understanding of reservoir optimization strategies but also have broader implications for sustainable water resource management, emphasizing the need for integrated approaches that consider both demand-side and supply-side interventions. Future research could explore additional factors such as environmental impacts and economic considerations to provide a more holistic understanding of the algorithm's applicability in real-world scenarios.

4. Conclusions

In conclusion, this research investigates the complexities of optimizing the operation of the Mujib Reservoir, recognizing the challenges posed by non-linear problems, multiple decision variables, and difficult-to-simulate constraints. The study employs Meta-Heuristic Algorithms (MHA), particularly the Charged System Search (CSS) algorithm, to address water deficit issues, considering scenarios such as sediment effects, water demand management, and increasing reservoir volume. The findings highlight the significant impact of sediment on reservoir capacity and the effectiveness of various strategies in mitigating water deficit. However, the study acknowledges limitations, including the abstraction introduced by MHA, uncertainties in sediment data extrapolation, and the need for more accurate information for precise simulations. The research considers for future exploration and improvement, emphasizing the importance of sensitivity analyses for algorithmic robustness, obtaining more accurate sediment data, and exploring alternative optimization algorithms. In addition, it includes for detailed socio-economic and environmental impact assessments, dynamic optimization models, and consideration of climate change projections. Furthermore, the research underscores the need for adapting strategies to different water inflow scenarios, addressing evaporation and seepage issues, and implementing effective water demand management. Comparative analysis, utilizing Risk analysis (volumetric reliability, shortage index (SI), resilience, vulnerability) and error indexes (correlation coefficient R2, the root mean square error (RMSE), and the mean absolute error (MAE)), evaluates results against the current operation. Sediment removal decreases water deficit by 19.42%, and considering sediment in the CSS algorithm reduces it by 9.7%. Water demand management scenarios show a 42.40% reduction in water deficit with reduced agricultural demand and sediment removal. Conversely, an increase in water demand leads to a 4.9% deficit increase. Increasing reservoir storage capacity by 10%, 20%, and 30%, coupled with sediment removal, results in deficit decreases of 26.50%, 32.14%, and 35.44%, respectively. Combining increased storage and reduced demand achieves deficit reductions of 47.90%, 51.41%, and 53.59%, offering viable solutions for decision-makers addressing water deficit in the reservoir. Despite the research's contributions, challenges in obtaining relevant economic data are acknowledged, with limitations in economic analysis rigor due to data scarcity and confidentiality constraints. In fact, there is a room for future research to address these challenges, exploring alternative data sources and relaxing confidentiality constraints to enable more robust insights into the economic dynamics of reservoir management.

CRediT authorship contribution statement

Sherif Mohsen: Writing – review & editing, Writing – original draft, Conceptualization. **A. Mahmoud Moamin:** Writing – review & editing, Writing – original draft. **El-Shafie Ahmed:** Writing – review & editing, Writing – original draft, Methodology, Investigation, Conceptualization. **Abid Almubaidin Mohammad Abdullah:** Writing – review & editing, Visualization, Validation, Software, Investigation, Data curation. **Malek Marlinda Binti Abdul:** Writing – review & editing, Writing – original draft. **Najah Ahmed Ali:** Writing – review & editing, Writing – original draft, Supervision, Conceptualization.

Declaration of Competing Interest

The authors declare that they have no known competing financial interests or personal relationships that could have appeared to influence the work reported in this paper.

Data availability

The authors do not have permission to share data.

Acknowledgments

This work was supported by the Ministry of Higher Education, Malaysia, through the Fundamental Research Grant Scheme (FRGS), under the project code of FRGS/1/2020/TK0/UNITEN/02/16.

References

Allawi, M.F., Jaafar, O., Mohamad Hamzah, F., Ehteram, M., Hossain, Md.S., El-Shafie, A., 2018. Operating a reservoir system based on the shark machine learning algorithm. Environ. Earth Sci. 77 (10), 366 https://doi.org/10.1007/s12665-018-7546-8.

Almubaidin, M.A., Latif, S.D., Balan, K., Ahmed, A.N., El-Shafie, A., 2023. Enhancing sediment transport predictions through machine learning-based multi-scenario

regression models. Results Eng., 101585 https://doi.org/10.1016/j.rineng.2023.101585.
Almubaidin, M.A.A., Ahmed, A.N., Sidek, L.B.M., Elshafie, A., 2022. Using Metaheuristics Algorithms (MHAs) to Optimize Water Supply Operation in Reservoirs: a Review. Arch. Comput. Methods Eng. 29 (6), 3677–3711. https://doi.org/10.1007/s11831-022-09716-9.
Al-Mubaidin, M., Al-Hamaiedeh, H., El-Hasan, T., 2022. Impact of the Effluent Characteristics of Industrial and Domestic Wastewater Treatment Plants on the Irrigated Soil and Plants. *Jordan J. Earth Environ. Sci.*
Arekhi, S., Shabani, A., Rostamizad, G., 2012. Application of the modified universal soil loss equation (MUSLE) in prediction of sediment yield (Case study: Kengir Watershed, Iran). Arab. J. Geosci. 5 (6), 1259–1267. https://doi.org/10.1007/s12517-010-0271-6.
Asadieh, B., Afshar, A., 2019. Optimization of Water-Supply and Hydropower Reservoir Operation Using the Charged System Search Algorithm. Hydrology 6 (1), 5. https://doi.org/10.3390/hydrology6010005.
Ashofteh, P.-S., Bozorg-Haddad, O., Loáiciga, H.A., 2020. Logical genetic programming (LGP) application to water resources management. Environ. Monit. Assess. 192 (1), 34 https://doi.org/10.1007/s10661-019-8014-y.
Ashofteh, P.-S., Bozorg-Haddad, O., Loáiciga, H.A., 2021. Application of bi-objective genetic programming for optimizing irrigation rules using two reservoir performance criteria. Int. J. River Basin Manag. 19 (1), 55–65. https://doi.org/10.1080/15715124.2019.1613415.
Azamathulla, H.Md, 2012. Gene expression programming for prediction of scour depth downstream of sills. J. Hydrol. 460–461, 156–159. https://doi.org/10.1016/j.jhydrol.2012.06.034.
Banadkooki, F.B., Adamowski, J., Singh, V.P., Ehteram, M., Karami, H., Mousavi, S.F., Farzin, S., EL-Shafie, A., 2020. Crow algorithm for irrigation management: a case study. Water Resour. Manag. 34 (3), 1021–1045. https://doi.org/10.1007/s11269-020-02488-6.
Bayesteh, M., Azari, A., 2021. Stochastic optimization of reservoir operation by applying hedging rules. J. Water Resour. Plan. Manag. 147 (2) https://doi.org/10.1061/(ASCE)WR.1943-5452.0001312.
Bekele, M., 2021. Geographic information system (GIS) based soil loss estimation using RUSLE model for soil and water conservation planning in anka_shashara watershed, southern Ethiopia. Int. J. Hydrol. 5 (1), 9–27. https://doi.org/10.15406/ijh.2021.05.00260.
Benavidez, R., Jackson, B., Maxwell, D., Norton, K., 2018. A review of the (Revised) Universal Soil Loss Equation ((R)USLE): with a view to increasing its global applicability and improving soil loss estimates. Hydrol. Earth Syst. Sci. 22 (11), 6059–6086. https://doi.org/10.5194/hess-22-6059-2018.
Bozorg-Haddad, O., Aboutalebi, M., Ashofteh, P.-S., Loáiciga, H.A., 2018. Real-time reservoir operation using data mining techniques. Environ. Monit. Assess. 190 (10), 594 https://doi.org/10.1007/s10661-018-6970-2.
Chamoun, S., De Cesare, G., Schleiss, A.J., 2016. Managing reservoir sedimentation by venting turbidity currents: A review. Int. J. Sediment Res. 31 (3), 195–204. https://doi.org/10.1016/j.ijsrc.2016.06.001.
Chong, K.L., Lai, S.H., Ahmed, A.N., Zaafar, W.Z.W., Rao, R.V., Sherif, M., Sefelnasr, A., El-Shafie, A., 2021. Review on Dam and Reservoir Optimal Operation for Irrigation and Hydropower Energy Generation Utilizing Meta-Heuristic Algorithms. IEEE Access 9, 19488–19505. https://doi.org/10.1109/ACCESS.2021.3054424.
Cimorelli, L., Covelli, C., De Vincenzo, A., Pianese, D., Molino, B., 2021. Sedimentation in Reservoirs: Evaluation of Return Periods Related to Operational Failures of Water Supply Reservoirs with Monte Carlo Simulation. J. Water Resour. Plan. Manag. 147 (1) https://doi.org/10.1061/(ASCE)WR.1943-5452.0001307.
Donyaii, A., Sarraf, A., Ahmadi, H., 2020. Water Reservoir Multiobjective Optimal Operation Using Grey Wolf Optimizer. Shock Vib. 2020, 1–10. https://doi.org/10.1155/2020/8870464.
Ehteram, M., Karami, H., Farzin, S., 2018. Reducing Irrigation Deficiencies Based Optimizing Model for Multi-Reservoir Systems Utilizing Spider Monkey Algorithm. Water Resour. Manag. 32 (7), 2315–2334. https://doi.org/10.1007/s11269-018-1931-7.
Farhan, Y., Nawaiseh, S., 2015. Spatial assessment of soil erosion risk using RUSLE and GIS techniques. Environ. Earth Sci. 74 (6), 4649–4669. https://doi.org/10.1007/s12665-015-4430-7.
Gong, Z., Cheng, J., Gong, Y., Wang, L., Wei, C., 2020. Modified particle swarm algorithm for the optimal water allocation of reservoir. Water Supply 20 (7), 2875–2883. https://doi.org/10.2166/ws.2020.188.
Hajiabadi, R., Zarghami, M., 2014. Multi-objective reservoir operation with sediment flushing; case study of Sefidrud Reservoir. Water Resour. Manag. 28 (15), 5357–5376. https://doi.org/10.1007/s11269-014-0806-9.
Hossain, M.S., El-Shafie, A., Mahzabin, M.S., Zawawi, M.H., 2018. System performances analysis of reservoir optimization–simulation model in application of artificial bee colony algorithm. Neural Comput. Appl. 30 (7), 2101–2112. https://doi.org/10.1007/s00521-016-2798-2.
Ijam, A.Z., Al-Nawiseh, A.N., & Ktishat, K., Storage Reduction of Mujeb Dam Reservoir in Jordan due to Sedimentation, 2020. *10*(6). https://doi.org/10.7176/jees/10–6-10.
Ijam, A., Al-Mahamid, M., 2012. Predicting sedimentation at Mujib dam reservoir in Jordan. Jordan Journal of Civil Engineering 6 (4), 448–463.
Jamshidi, J., Shourian, M., 2019. Hedging Rules-Based Optimal Reservoir Operation Using Bat Algorithm. Water Resour. Manag. 33 (13), 4525–4538. https://doi.org/10.1007/s11269-019-02402-9.
Kalhori, M., Ashofteh, P.-S., Moghadam, S.H., 2023. Development of the Multi-Objective Invasive Weed Optimization Algorithm in the Integrated Water Resources Allocation Problem. Water Resour. Manag. 37 (11), 4433–4458. https://doi.org/10.1007/s11269-023-03564-3.
Karami, H., Mousavi, S.F., Farzin, S., Ehteram, M., Singh, V.P., Kisi, O., 2018. Improved Krill Algorithm for Reservoir Operation. Water Resour. Manag. 32 (10), 3353–3372. https://doi.org/10.1007/s11269-018-1995-4.
Kaveh, A., Talatahari, S., 2010. A novel heuristic optimization method: charged system search. Acta Mech. 213 (3–4), 267–289. https://doi.org/10.1007/s00707-009-0270-4.
Khan, N.M., Babel, M.S., Tingsanchali, T., Clemente, R.S., Luong, H.T., 2012. Reservoir Optimization-Simulation with a Sediment Evacuation Model to Minimize Irrigation Deficits. Water Resour. Manag. 26 (11), 3173–3193. https://doi.org/10.1007/s11269-012-0066-5.
Khassaf, S., al Rammahi, A., 2018. Estimation of slope length factor (L) and slope steepness factor (S) of rusle equation in the euphrates river watershed by gis modeling. Kufa J. Eng. 9 (3), 81–91. https://doi.org/10.30572/2018/kje/090307.
Kumar, V., Yadav, S.M., 2020. Optim. Water Releases Ukai Reserv. Using Jaya Algorithm 323–336. https://doi.org/10.1007/978-981-13-8196-6_29.
Loucks, D.P., van Beek, E., 2017. Water Resource Systems Planning and Management. Springer International Publishing,. https://doi.org/10.1007/978-3-319-44234-1.
Md. Azamathulla, H., Wu, F.-C., Ghani, A.A., Narulkar, S.M., Zakaria, N.A., Chang, C.K., 2008. Comparison between genetic algorithm and linear programming approach for real time operation. J. Hydro-Environ. Res. 2 (3), 172–181. https://doi.org/10.1016/j.jher.2008.10.001.
Mendoza Ramírez, R., Arganis Juárez, M.L., Domínguez Mora, R., Padilla Morales, L.D., Fuentes Mariles, Ó.A., Mendoza Reséndiz, A., Carrizosa Elizondo, E., Carmona Paredes, R.B., 2021. Operation Policies through Dynamic Programming and Genetic Algorithms, for a Reservoir with Irrigation and Water Supply Uses. Water Resour. Manag. 35 (5), 1573–1586. https://doi.org/10.1007/s11269-021-02802-w.
Moeini, R., Soghrati, F., 2020. Optimum outflow determination of the multi-reservoir system using constrained improved artificial bee colony algorithm. Soft Comput. 24 (14), 10739–10754. https://doi.org/10.1007/s00500-019-04577-0.
Moghadam, S.H., Ashofteh, P.-S., Loáiciga, H.A., 2022. Optimal Water Allocation of Surface and Ground Water Resources Under Climate Change with WEAP and IWOA Modeling. Water Resour. Manag. 36 (9), 3181–3205. https://doi.org/10.1007/s11269-022-03195-0.
Neitsch, S.L., Arnold, J.G., Kiniry, J.R., Williams, J.R., 2011. Coll. AGRICULTURE LIFE Sci. Soil Water Assess. Tool. Theor. Doc. Version 2009.
Patle, B.K., Parhi, D.R., Jagadeesh, A., Kashyap, S.K., 2017. On firefly algorithm: optimization and application in mobile robot navigation. World J. Eng. 14 (1), 65–76. https://doi.org/10.1108/WJE-11-2016-0133.
Qaderi, K., Akbarifard, S., Madadi, M.R., Bakhtiari, B., 2018. Optimal operation of multi-reservoirs by water cycle algorithm. Proc. Inst. Civ. Eng. - Water Manag. 171 (4), 179–190. https://doi.org/10.1680/jwama.16.00034.
Shi, P., Zhang, Y., Ren, Z., Yu, Y., Li, P., Gong, J., 2019. Land-use changes and check dams reducing runoff and sediment yield on the Loess Plateau of China. Sci. Total Environ. 664, 984–994. https://doi.org/10.1016/j.scitotenv.2019.01.430.
Su, G., Xu, S., Liu, Y., Yu, H., Mu, B., 2022. Sediment Distribution and Treatment in the Inflow Water-Level-Fluctuating Zone of the Biliuhe Reservoir. Water 14 (4), 580. https://doi.org/10.3390/w14040580.
Williams, J.R., 1975. Sediment-yield Prediction with Universal Equation using Runoff Energy Factor. US Department of Agriculture,, Washington, DC.
Wischmeier, W.H., S. D. D, 1978. Predicting Rainfall-Erosion Losses- A Guide To Conservation Planning. USDA Agriculture Handbook 573. U.S. Gov. Print. Office,, Washington, D.
Yaseen, Z.M., Allawi, M.F., Karami, H., Ehteram, M., Farzin, S., Ahmed, A.N., Koting, S. B., Mohd, N.S., Jaafar, W.Z.B., Afan, H.A., El-Shafie, A., 2019. A hybrid bat–swarm algorithm for optimizing dam and reservoir operation. Neural Comput. Appl. 31 (12), 8807–8821. https://doi.org/10.1007/s00521-018-3952-9.
Yin, X.-A., Yang, Z.-F., Petts, G.E., Kondolf, G.M., 2014. A reservoir operating method for riverine ecosystem protection, reservoir sedimentation control and water supply. J. Hydrol. 512, 379–387. https://doi.org/10.1016/j.jhydrol.2014.02.037.
Zhang, D., Peng, Q., Lin, J., Wang, D., Liu, X., Zhuang, J., 2019. Simulating reservoir operation using a recurrent neural network algorithm. Water 11 (4), 865. https://doi.org/10.3390/w11040865.